EFFECT OF PROCESS PARAMETERS ON THE MECHANICAL PROPERTIES OF 3D-PRINTED PLA PARTS USING FUSED DEPOSITION MODELING PROCESS

A thesis submitted towards partial fulfilment of the requirements for the degree of

Master of Technology in Laser Technology

Course affiliated to Faculty of Engineering and Technology, Jadavpur University

Submitted by

SABYASACHI DEY

Examination Roll No.: M4LST23004

Registration No. 160424 of 2021-22

School of Laser Science and Engineering

Faculty of Interdisciplinary Studies, Law and Management

Jadavpur University

Kolkata -700032

India

2023

JADAVPUR UNIVERSITY

FACULTY OF INTERDISCIPLINARY STUDIES, LAW AND MANAGEMENT

CERTIFICATE OF RECOMMENDATION

I HERE BY RECOMMEND THAT THE THESIS PREPARED UNDER MY SUPERVISION BY **SABYASACHI DEY** ENTITLED **EFFECT OF PROCESS PARAMETERS ON THE MECHANICAL PROPERTIES OF 3D-PRINTED PLA PARTS USING FUSED DEPOSITION MODELING PROCESS** BE ACCEPTED IN THE PARTIAL FULFILLMENT OF THE REQUIREMENTS FOR THE DEGREE OF MASTER OF TECHNOLOGY IN LASER TECHNOLOGY DURING THE ACADEMIC SESSION 2021-2023.

THESIS SUPERVISOR
DR. PARAMASIVAN K
School of Laser Science and Engineering
Jadavpur University, Kolkata-700032

CO - SUPERVISOR
Sri. SUKANTA SAHA
Assistant Professor
School of Mechanical Engineering
Heritage Institute of Technology, Kolkata-700107

Countersigned

DIRECTOR
Dipten Misra
School of Laser Science and Engineering
Jadavpur University, Kolkata-700 032

DEAN
Faculty of Interdisciplinary Studies, Law and Management
Jadavpur University, Kolkata-700 032

JADAVPUR UNIVERSITY

FACULTY OF INTERDISCIPLINARY STUDIES, LAW AND MANAGEMENT

CERTIFICATE OF APPROVAL **

This foregoing thesis is hereby approved as a creditable study of an engineering subject carried out and presented in a manner satisfactory to warrant its acceptance as a prerequisite to the degree for which it has been submitted. It is understood that by this approval the undersigned do not necessarily endorse or approve any statement made, opinion expressed or conclusion drawn therein but approve the thesis only for the purpose for which it has been submitted.

COMMITTEE OF FINAL EXAMINATION FOR EVALUATION OF THESIS

** Only in case the recommendation is concurred

DECLARATION OF ORIGINALITY AND COMPLIANCE OF ACADEMIC ETHICS

The author hereby declares that this thesis contains original research work by the undersigned candidate, as part of his Master of Technology in Laser Technology studies during the academic session 2019-2021.

All information in this document has been obtained and presented in accordance with academic rules and ethical conduct.

The author also declares that as required by this rules and conduct, the author has fully cited and referred to all material and results that are not original to this work.

NAME: SABYASACHI DEY

EXAMINATION ROLL NUMBER: M4LST23004

THESIS TITLE: EFFECT OF PROCESS PARAMETERS ON THE MECHANICAL PROPERTIES OF 3D-PRINTED PLA PARTS USING FUSED DEPOSITION MODELING PROCESS.

31/07/2023

SIGNATURE

ACKNOWLEDGEMENT

First and foremost, I would like to express my sincere gratitude to my supervisor **Dr. Paramasivan K**, School of Laser Science and Engineering, Jadavpur University and **Prof. Dipten Misra**, Director, School of Laser Science and Engineering, Jadavpur University, for his invaluable guidance, whole-hearted support and encouragement for accomplishing the present investigation. His dynamism, fantastic stamina and day-to-day monitoring in every minute detail were a constant source of inspiration to me.

I am extremely thankful to **Prof. Sanjib Acharyya**, Department of Mechanical Engineering, Jadavpur University, for giving me the opportunity to use the laboratory facilities.

I am extremely thankful to my co-supervisor **Sukanta Saha**, my senior and my friends of School of Laser Science and Technology, for their inspiration and encouragement and helping me through the research work.

I record my acknowledgement to **School of Laser Science and Engineering** for giving me the opportunity to pursue my research work.

Immemorial friendly behaviour and constant support of all my friends, seniors and juniors of School of Laser Science and Engineering are highly acknowledged.

All staff members of School of Laser Science and Technology deserve special thanks for their help in diverse ways during the days of my stay in the department.

No words can convey my sense of gratitude for my family.

SABYASACHI DEY
Examination Roll No. M4LST23004
Registration No. 160424 of 2021-2023

This thesis work is dedicated to:

My beloved mother Smt. Sima Dey, My beloved father Sri. Harish Chandra Dey My respected Sir Paramasivan K., Sukanta Saha and Dipten Misra.

TABLE OF CONTENTS

ACRONYMS

SLA: Sterolithography Apparates

CLIP: Continuous Liquid Interface Production

DOD: Drop on Demand

FDM: Fused Deposition Modeling

FFF: Fused Filament Fabrication

LOM: Laminated Object Manufacturing

SLM: Selective Laser Melting

SLS: Selective Laser sintering

EBM: Electron Beam Melting

DMLS: Direct Metal Laser Sintering

LENS: Laser Energy Net Shaping

EBW: Electron Beam Welding

LIST OF FIGURES

LIST OF TABLES

ABSTRACT

EFFECT OF PROCESS PARAMETERS ON THE MECHANICAL PROPERTIES OF 3D-PRINTED PLA PARTS USING FUSED DEPOSITION MODELING PROCESS

Fused Deposition Modeling is fourth type of Additive Manufacturing based on energy consumption. Fused deposition modelling or fused filament fabrication also well known as Material Extrusion is a commonly used additive manufacturing process for aerospace, automobile and polymer industry. The following 3D printing process factors will enhance the mechanical qualities of 3D printed products: Nozzle size, Filament size, melting temperature, Bed heat, Printing Speed, Layer thickness, Infill geometry, Number of Layers, Raster angle, Raster gap, and Raster width. ASTM D 638 type IV specimen is selected for this experiment. PLA, which has a low melting point and little warping is used in this experiment. To control that warping bed temperature (30℃) takes an important role to print the specimen. Two process parameters are selected, those are path width and raster angle, which have also an effect on tensile strength of PLA samples. Path width is the main process parameters in this study. The object of this study is to determine the mechanical properties of ASTM D 638 type IV standard specimen with varying the path width. Due to that path width, there was an overlapping when the material is extracted from the nozzle. The effect of longitudinal overlapping of type IV specimen is observed. We get the maximum tensile strength of 46.075 MPa at 15% overlapping. ASTM standards provide guidelines and specifications for various materials and testing procedures. However, specific standards for 3D printing with PLA may not explicitly mention raster angle or path width because it is more related to the printing process and machine parameters. Nonetheless, ASTM standards often include mechanical testing requirements, including UTS measurements, which can be indirectly influenced by factors such as raster angle, path width.

CHAPTER I
INTRODUCTION

1. General Introduction

Manufacturing involves the use of resources like machinery, labour, tools, chemicals, or biological formulations to create items. This is the foundation of the economy's secondary sector and can refer to various human endeavours, from handicraft to high-tech. However, it is most commonly associated with industrial design, which involves transforming raw materials from the primary sector into finished commodities. These commodities can be distributed through the tertiary industry to end-users and customers or sold to other manufacturers for the creation of more advanced products. The field of engineering known as "manufacturing engineering" is responsible for planning and optimizing the steps involved in turning raw materials into finished goods. The production process begins with product design and material requirements and concludes with the creation of the final product by manufacturing these materials into various forms.

1.1 Historical Background

Various Additive Manufacturing (AM) technologies are now making it possible to produce both functional prototypes and finished products. These technologies share many functional similarities despite being very different in their solutions, underlying principles, and implementations. The primary data to support this dynamic analysis comes from the publications. The following are the most significant from a chronological perspective:

The 1940s

In his short story "Things Pass By" in 1945, Murray Leinster presented the main concept and process of 3D printing. However, the versatility of the technology and efficiency are highlighted in Raymond F. Jones' "Tools of the Trade" in the November 1950 edition of Astounding Science Fiction magazine.

The 1970s

Johannes F. Gottwald invented the Liquid Metal Recorder, U.S. Patent 3596285A, which is a device that uses continuous inkjet technology to create a detachable metal fabrication on a reusable surface. The metal can be remelted and reused for immediate printing or saved for future use. This patent appears to be the earliest mention of 3D printing with controlled pattern manufacturing and rapid prototyping.

The 1980s

Additive manufacturing machinery and materials are first developed in the 1980s. Hideo Kodama created two techniques for producing three-dimensional plastic models with photo-hardening thermoset polymers in April 1980. These techniques involve controlling the UV exposure region with a mask pattern or scanning fibre transmitter. Kodama submitted a patent for his XYZ plotter, which is published on November 10th, 1981. Raytheon Technologies Corp is issued a patent entitled "Method of fabricating articles by sequential deposition" in the US on April 6, 1982, which is an early example of the formation of "layers" and fabrication of objects on a substrate. American businessman Bill Masters submitted a patent application on July 2, 1984, for his computer automated manufacturing process and system. UVP, Inc. filed a patent application for their own stereo lithography fabrication system on August 8, 1984, which involves adding individual laminate or layers by curing photopolymers with impinging radiation, particle bombardment, chemical reaction, or ultraviolet light lasers.

The 1990s

In the mid-1990s, Stanford University and Carnegie Mellon University developed new methods for material deposition, including micro casting and sprayed materials. There is also an increase in availability of support and sacrifice materials, allowing for new object geometries. At MIT in 1993, Emanuel Sachs invented a powder bed method using inkjet print heads, which is later commercialized by Soligen Technologies, Extrude Hone Corporation, and Z Corporation, and gave rise to the term "3D printing." Sanders Prototype, Inc. (later Solidscape) is founded in 1993 as the first inkjet 3D printer firm, and unveiled high-precision polymer jet production technology with soluble support structures. In 1995, the Fraunhofer Society invented the selective laser melting procedure, which is later patented by Chuck Hull of 3D Systems Corporation.

The 2000s

In 2009, the patents for Fused Deposition Modelling (FDM) printing method expired. This allowed new businesses to create commercial FDM 3D printers, many of which are inspired by the RepRap community. As additive processes developed, it is clear that metal removal would not be the only metalworking activity carried out by a tool or head moving through a 3D work envelope, layer by layer shaping a mass of raw material into the desired shape. The

technology has advanced to the point where some researchers are predicting that 3D printing could contribute to sustainable development in less developed countries.

The 2010s

In 2012, Filabot developed a mechanism that allowed for the use of a wider range of plastics in 3D printing through FDM or FFF printers. FDM is a popular 3D printing process that involves material extrusion and makes up 46% of all 3D printing processes as of 2018. Despite being developed after the commonly used technologies of SLA and SLS, FDM remains popular due to its affordability.

The 2020s

By the year 2020, the majority of people will have access to 3D printers due to their improved quality and affordability. Entry-level printers of decent quality will be available for purchase at a price of less than $200 USD, with most of them using Fused Deposition Modelling (FDM). In November 2021, Moorfields Eye Hospital in London presented the world's first fully 3D-printed prosthetic eye to a patient named Steve Verze from the United Kingdom.

1.2 Principle of Additive Manufacturing

Additive Manufacturing is a process that involves layer-by-layer addition of material to create a product within a short period of time while minimizing material waste. A design must be created before using this method, which can be done through Computer Aided Design (CAD) software or by scanning the object. The design is then converted into a framework for the additive manufacturing machine and transferred to the 3-D printer for production. The American Society for Testing and Materials (ASTM) defines additive manufacturing as the process of building objects by layering materials using digital data from CAD. This method involves melting, fusing, sintering, or polymerizing materials to create objects, similar to building a brick house. The quality of the product depends on the thickness of each layer, and thicker layers result in faster production. The model is saved in the STL file format and then sliced using a "slicer" program, which selects the necessary process parameters. Finally, a G-code file is produced and used to print the object using a 3D printer. In additive manufacturing, there are fewer manufacturing steps and the process goes as follows:

1. Design
2. Pre-processing to ensure the design can be printed

3. Iterate
4. Manufacture

1.3 Steps of Additive Manufacturing

Additive manufacturing, also known as 3D printing, is a computer-controlled procedure for creating 3D objects. This process involves adding material, such as plastic, ceramic, or metal powder, to a build platform in thin layers and then cementing the layers using a curing agent, heat, or a laser beam. Although the process is more complicated, there are four key steps to it. The flowchart of additive manufacturing process is shown in Figure 1.1.

Fig. 1.1 Process flowchart of AM

Step 1: Using CAD Software to Design a Model

Computer Aided Design (CAD) is crucial in additive manufacturing as it is used to create and test 3D models that are practical for real-world use. AutoCAD, Creo, and SolidWorks are some of the best CAD softwares used for commercial purposes.

1. AutoCAD is widely used in many industries for 3D design and is known for its flexibility.
2. Creo is a leader in product design with a wide range of design features and the ability to do dimension calculations throughout the modelling process.
3. SolidWorks is commonly used in industrial object design and includes a variety of engineering tools and functionality.

Step 2: Pre-Processing

Pre-processing refers to a variety of operations required between design and production. It includes two important activities.:

a) ***Simulation Modeling***

Simulation modelling is used for digital testing of 3D designs before production to assess the structural integrity of an object. This helps to determine whether it is likely to fail, how it might fail, and the amount of pressure it can withstand without failing. Common simulation

modelling methods include computational fluid dynamics (CFD), finite element analysis (FEA), and non-linear stress analysis.

b) ***Preparing Files for 3D printing***

Once a 3D design is reviewed, tested, and approved, it is ready for printing. However, there is a need for interoperability in order to achieve this. This means that different computer systems must be able to communicate and use information in order to work together. A challenge in additive manufacturing is that basic manufacturing equipment, such as 3D printers, struggle to interpret CAD files accurately. To overcome this issue, the CAD file must be transformed into a set of instructions that the hardware for additive manufacturing can understand. This is accomplished using 'Slicer' software, like Spatial's CGM Polyhedra, which converts the 3D design into 2D layers or slices. These slices are then used to determine the tool path or G-Code required to manufacture the product.

c) ***Printing***

The process of printing can vary greatly depending on the method of additive manufacturing used. For example, in 3D printing, a layer of binding liquid is alternated with a layer of powder material to create the final output. This technique is called "binder jetting". Stereo lithography (SLA) uses photopolymer resin that is cured by lasers instead of liquid binder, with each layer being printed onto the resin as the building platform is lowered into a resin pool. Fused Deposition Modelling (FDM) heats and deposits thermoplastic material layer by layer, while in Selective Laser Sintering (SLS), Metal Laser Sintering (DMLS), and Electron Beam Melting (EBM), different techniques are used to create the final product.

d) ***Post Processing***

Post-processing is often the most expensive and time-consuming aspect of additive manufacturing. The specific phases of post-processing vary depending on the type of additive manufacturing process used, but they generally fall into three categories.

1. Build removal - Removing extra material from the build platform and object.
2. Separation of parts - separation of parts, removal of the object from the assembly platform and dismantling of all building supports present.
3. Binder removal - Objects must be immersed in the solution to remove excess binders.

1.4 Classification of Additive Manufacturing

Based on ASTM standards, there are seven types of additive manufacturing,namely Vat Photopolymerization, Material Jetting, Binder Jetting, Material Extrusion, Sheet Lamination, Powder Bed Fusion, and Direct Energy Deposition.Classification of AM based on American Society for Testing and Materials (ASTM) standards is shown in Figure 1.2.

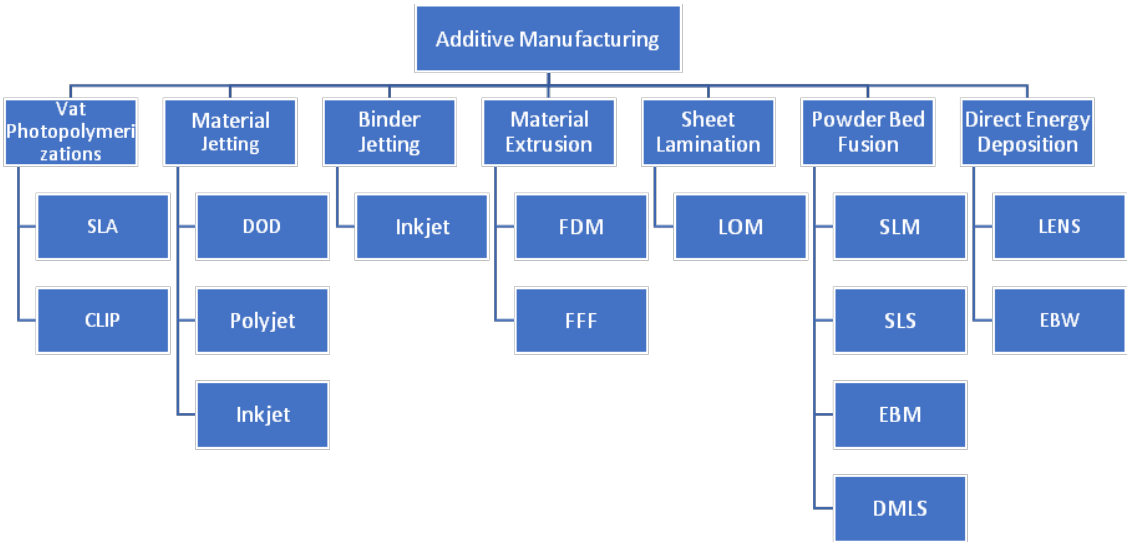

Figure 1.2 Classification of AM based on ASTM standards

a) ***Vat Photo polymerizations (Stereolithography)***

In 1986, Chuck Hull acquired a patent for the Stereolithography (SLA) method, which uses light to solidify liquid materials in a process called Photopolymerization. This involves exposing a Vat of liquid polymer to safelight lighting controls, causing cross-linking to occur and resulting in solidification. Photopolymerization occurs when chromophores are present, otherwise, photosensitive molecules are added to initiate the process. The addition of monomers leads to cross-linking, which alters the solution's properties. This process is repeated until the model is complete. The Envision TEC Perfactory is a DLP rapid prototyping system used for this purpose. Once finished, the solid model is removed from the vat along with the liquid polymer.

b) ***Material Jetting***

A nozzle filled with liquid can be used to remove liquid from an absorbent surface through wicking, from a larger orifice through electrostatic attraction, as a stream through pressurization, or in bursts through fluid pressure surges. Fountain pens and hoses are examples of wicking and streaming, respectively, while pumps can eject droplets or spray. Nozzles can be single or multi-chambered and made from any material, and are commonly found in inkjet printers. Only low viscosity ink can pass through the nozzle, but hot-melt inks can be melted to create liquid. Inkjet inks must be three-dimensional for creating a Z height component in 3D printing. Inkjet technology is invented by Teletype in 1966 with their Inktronic teleprinter, which printed at a record-breaking speed of 120 characters per second using 40 jets.

c) ***Binder Jetting***

The binder jetting 3D printing technique involves depositing a binding adhesive substance onto layers of typically powdered material, using metal or ceramic-based materials. This technique is also referred to as the "inkjet 3D printing system." The printer creates the model by spreading a layer of powder and printing a binder on each layer using a method similar to inkjet printing. The process is repeated for each layer, allowing for the creation of full-colour prototypes, overhangs, and elastomer pieces. To increase the durability of bonded powder prints, wax or impregnation with thermoset polymer may be used.

d) ***Material Extrusion***

Fused Deposition Modelling involves the extrusion of tiny beads or streams of material that quickly harden into layers to create a model or part. A thermoplastic filament or other low melting point material or mixture is fed into a nozzle head in a 3D printer extruder, where it is heated to melting point and extruded onto a build table. Alternatively, fused pellet deposition can be used, which employs plastic pellets or particles instead of filament. The substance is heated by the nozzle head, which also controls the flow. The extrusion head and flow control are typically accomplished using stepper or servo motors, and the G-Code is produced by a CAM software programme and delivered to a microcontroller that controls the motors.

Plastic is the most commonly used material for printing, and there are various polymers like Acrylonitrile Butadiene Styrene (ABS), Polycarbonate (PC), Polylactic Acid (PLA), High-density Polyethylene (HDPE), PC/ABS, Polyphenylsulfone (PPSU), and High Impact Polystyrene (HIPS) that can be utilized. Typically, these polymers are shaped into filaments made from new resins.The open-source community is developing ways to turn recycled

plastic into filament using recyclebots. Additionally, fluoropolymers like PTFE tubing are used for their high temperature resistance. One specific use for this process is transferring filaments. Schematic diagram of FDM is shown in Figure 1.3.

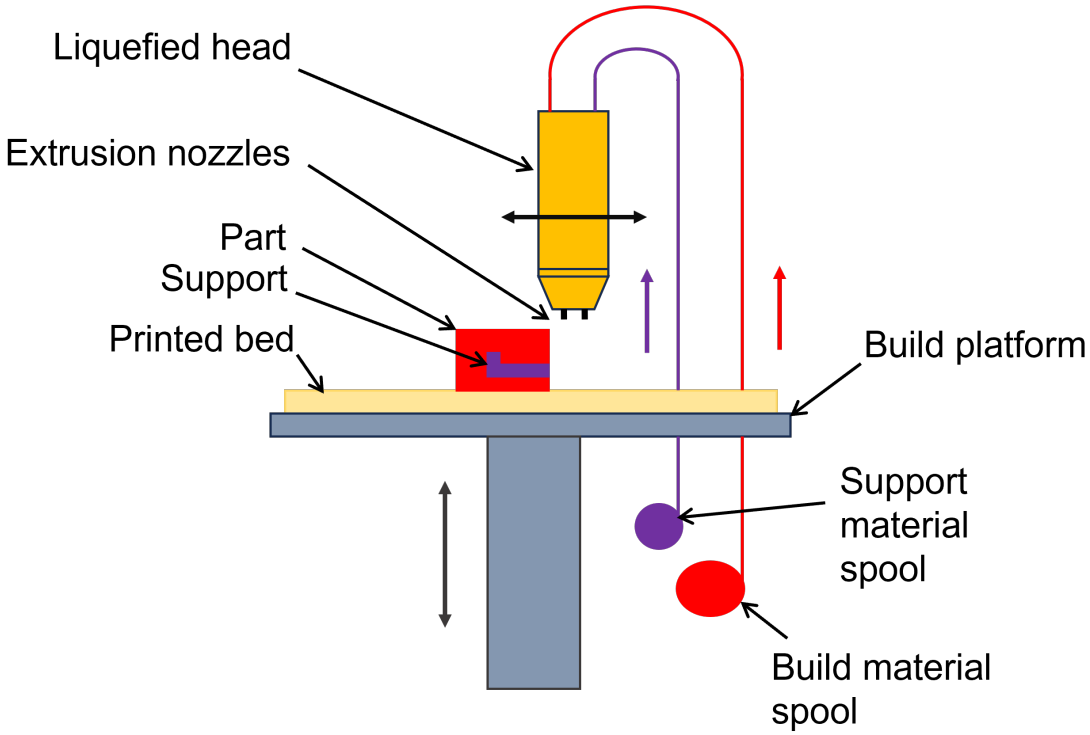

Fig.1.3 Schematic diagram of FDM

e) ***Sheet Lamination***

Using paper as the construction material in some printers can bring down printing costs. In the 1990s, certain businesses sold printers that used a carbon dioxide laser to cut cross sections from specially coated adhesive paper, which are then laminated. In 2005, Mcor Technologies Ltd. developed a different approach that involved using regular office paper sheets, a tungsten carbide blade to cut the shape, and pressure and selective adhesive deposition for connecting the prototype. Some businesses also offer printers that create laminated objects using thin metal and plastic sheets. Ultrasonic consolidation (UC) or ultrasonic additive manufacturing (UAM) is a low-temperature 3D printing or additive manufacturing technique for metals.

f) ***Powder Bed Fusion***

Selective material fusion is a 3D printing technique that involves melting parts of a layer, adding another layer of granules, and repeating the process until the object is complete. This method allows for thin walls and overhangs in the object without the need for temporary supports. Selective heat sintering is an example of this technique, where layers of powdered thermoplastic are heated and sintered to create the model. This method is less expensive than using a laser and can be used on smaller scales.

g) ***Direct Energy Deposition***

In powder-fed directed-energy deposition, metal powder will be melted using a high intensity laser. The laser beam will be focused by one or more lenses and is directed towards the centre of the deposition head. An X-Y table will be used to build the object layer by layer, and a digital model is used to generate the tool path. As each layer is completed, the deposition head can be raised vertically. Some systems use 5- or 6-axis systems to transfer material with no spatial limits. Metal powder can be delivered by nozzles positioned in different configurations around the deposition head. A hermetically sealed chamber filled with inert gas or a local inert shroud gas can be used to shield the melt pool from oxygen. The technique is similar to selective laser sintering, as it only projects metal powder where it is being added to the part. This method is compatible with a variety of materials, including composites and functionally graded material, as well as titanium, stainless steel, aluminium, tungsten, and other specialised materials. Figure 1.4 shows the selection of the additive manufacturing process based on raw materials.

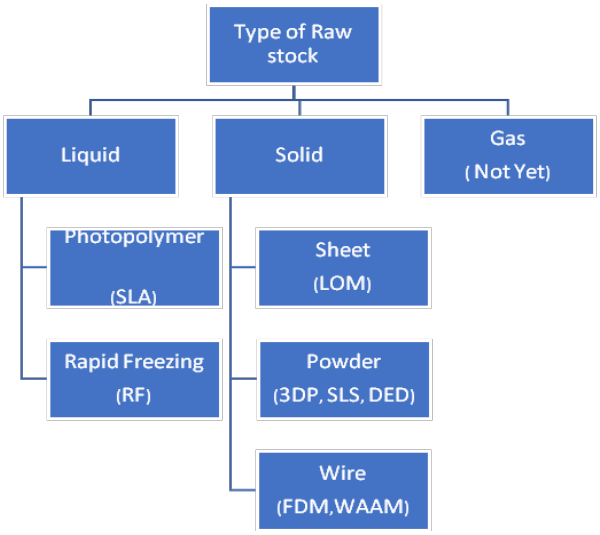

Figure 1.4 Selection of the additive manufacturing process based on raw materials.

1.5 Application of Additive Manufacturing

The production of 3D printed objects has moved from research and development to additive manufacturing technology. This technology allows for the creation of concepts that are previously unachievable in the manufacturing industry. Additive manufacturing is a powerful and diverse method that is becoming increasingly important in various industrial sectors, playing a crucial role in Industry 4.0.

1. **Aerospace**
    a) 3D Printed Rapid Prototypes for Functional Rocket Testing
    b) Create Complex Rocket Parts With 3D Printing
    c) Prototyping Aerospace Tooling With 3D Printing
    d) Create Light weight Components.
    e) Build Parts with Complex Geometries.

2. **Automobile**
    a) Rapid Prototyping
    b) Production of Lightweight Hinges & Brackets
    c) Production of Engine Parts
    d) Production of Cooling Systems
    e) Production of Heat Exchangers and Gears

3. **Pharmaceutical**
    a) Production of Medical Equipment
    b) Drug delivery system
    c) Living tissue and organ printing.
    d) production of orthopaedic implants

4. **Naval**
    a) Production of Naval Vessels
    b) Production of Pass Anger
    c) Making boat hulls
    d) Production of Gas mask
    e) Production of Life boats

Additionally, this technology is utilized in various sectors such as education, firearm, fashion, food, construction for building houses and small bridges, passenger waiting rooms, as well as sports and toy industries.

1.6 Advantage and Limitation of Additive Manufacturing

1. **Advantages**
    a) Major waste reduction aspect
    b) The ability to produce customised or specially made parts
    c) A reduction in lead times
    d) Increased energy efficiency
    e) The ability to produce components with a high strength-to-weight ratio
    f) Improved accuracy and repeatability

2. **Limitations**
    a) High cost of equipment and materials
    b) The need for skilled operators
    c) Limited choice of materials
    d) The slow speed of the process
    e) The need for post-processing (sintering, heat treatment, etc.)

CHAPTER II
LITERATURE REVIEW

2.1 Review of Past Research

Additive manufacturing covers a wide range of techniques that vary depending on the material, energy source, and method used. Both metal and non-metal products can be produced using different methods. This section evaluates the literature on the material extrusion process and fused deposition modelling (FDM), which is also referred to as fused filament fabrication or a wire-based additive manufacturing technique. The section further investigates the effects of the FDM process parameters on the product development and printed product properties.

2.2 Review of Literature on Additive Manufacturing

Vaught *et al*. [1] examined the wear resistance of items produced through additive manufacturing. They found that when processed using fused deposition modelling, glycol-modified polyethylene terephthalate showed a lower wear rate compared to virgin material when exposed to slow-speed dry sliding contact. This is a unique example of an additive-manufactured material with improved bulk properties.

Basha *et al*. [2] utilized the AFF method to examine how deballing and surface finish improvement occurs on 18Ni300 steel made through selective laser melting. They found that using an abrasive medium with a bimodal distribution of abrasive particles led to greater material removal and surface roughness reduction compared to a monomodal abrasive medium. The bimodal abrasive medium resulted in a reduction of surface roughness by up to 93%.

Herrera *et al*. [3] examined the wear of Ti-6Al-4V titanium alloys using the ASTM G65 test method. They used both traditional and EBM techniques and found that the EBM specimens exhibited over twice as much wear as the traditionally produced specimens, along with considerably more scratches.

Niu *et al*. [4] investigated the combination of Wire Arc Additive Manufacturing (WAAM) and Laser Cladding (LC) to create 304 components with a reinforced TiC ceramic coating. The research illustrates that the hybrid method can produce ceramic-metal matrix composites with intricate structures. This approach could offer a fresh approach to manufacturing integrated components with unique structural elements and surface performance requirements.

Chen *et al*. [5] examined the microstructure and mechanical properties of Inconel 625 produced through selective laser melting (SLM) and laser engineered net shaping (LENS) methods. The dislocation density of SLM-printed Inconel 625 is significantly higher, at

$2.8\pm1.2\times 10^{14}$ m^{-2}. The difference in yield strength between SLM and LENS printed Inconel 625 is primarily attributed to distinct dislocation strengthening effects.

Zhang *et al*. [6] studied the slurry-based laminated object production method for creating porous ceramics. They asserted that utilizing an organic mesh as the structure and template reduces the risk of damage to the green body and guarantees the uniformity, stability, and connection of the pore network at the micron scale.

Lu *et al*. [7] conducted a study on how the size of powder affects the number of whiskers. They suggested that their methodology can be applied in controlling the microstructure of in-situ whiskers through SLS technology, as well as in other 3D printed ceramic material systems that require in-situ reinforcement with whiskers.

Zhang *et al*. [8] successfully 3D printed high-performance graphene/polymer composites using vat photopolymerization. These composites exhibit excellent electrical conductivity, mechanical strength, and thermal stability. The researchers used a photo/thermal dual-curing polymer matrix and found that this method not only enabled continuous manufacturing of the composites, but also improved their electrical conductivity, strength, and ductility.

Liu *et al.* [9] utilized a snap-fit method in combination with PolyJet technology to produce polymer lattice structures. They observed that reducing the thickness of the struts resulted in the snap-fitted lattices exhibiting greater strength advantages over their integrated counterparts. Furthermore, the compressive peak strengths of the PolyJet lattices that were snap-fitted can be estimated by utilizing ideal maximum strength models that are based on yielding, elastic buckling, and inelastic buckling.

Shokraneh*et al.* [10] investigated the application of contactless Magneto Hydro Dynamic (MHD) Drop-On-Demand (DOD) actuation in 3D printing of 7075-aluminium alloy using liquid metal. They evaluated the impact of various actuation parameters, including Hartmann number, Strouhal number, pulse width ratio and waveform, on the droplet production process by analyzing sub-models against experimental and analytical benchmarks.

Based on F-42 committee seven different types of additive manufacturing process, there advantage and limitation are given below in Table 2.1.

Table 2.1 Additive Manufacturing process, there advantage and limitation

Process	Advantage	Limitation
Vat Polymerization	- A high degree of detail, precision and overall quality. -The process is rather rapid.	- Lack of photo-resin material choices. - Resins can warp and bend over time.
Material Jetting	- High Resolution due to nanoscale jetting. -Very nice surface finish. - Safer and easier to handle with no loose powder.	- parts are very expensive. - Very slow process. - Most applications limited to small parts.
Binder Jetting	- The two-material method allows for many different binder powder combinations and various mechanical properties. - Parts can be made in a range of different colours.	- Not always suitable for structural parts due to the use of binder material. - Additional post processing can add significant time to the overall process.
Material Extrusion	- Budget Friendly - Filament Reusable - Cloud server printing - Easily portable	- Rough surface finishing - Warping is common - Nozzle clogging - Weak in strength
Sheet Lamination	- Faster print time - No support structures required - Multi material layers possible - Ability to integrate hybrid manufacturing system	- Layer height cannot be changed without changing the sheet thickness - Limited material options available - Material west can also be very high

Powder Bed Fusion	- Reduced material waste - Improved manufacturing times - Flexibility - Efficient recycling of un-melted powder	- Relatively slow and long printing time - Weak structural properties - High power usage
Direct energy Deposition	- Complex geometries - Reduces the material waste - Possibility of deposit functional and graded materials. - In situ alloying	- Distortions, porosity, and inhomogeneities - Low part quality and accuracy - High production time - High cost of raw materials

2.3 Review of Literature on Fused Deposition Modeling

Smart Manufacturing is the most efficient way to bring about an industrial revolution. Additive Manufacturing, specifically 3D printing, is a process that allows for precise production of products. While it can be time-consuming, we can design different .stl files for a single product based on our needs and the cost of the product. There are various parameters involved in the 3D printing process, including geometry-based parameters, process parameters, and structural-based parameters. Utilizing all materials without generating waste is a major achievement of 3D printing.

B.M. Tymrak [11] has shown that components produced by 3D printing have mechanical properties such as elastic modulus and tensile strength that are similar to those produced by commercial 3D printing.Standard tensile tests are conducted on PLA and ABS components produced using RepRap 3D printers, which are open-source and self-replicating. The tests aim to determine elastic modulus, tensile strength, and strain at maximum strength. Some printed structures demonstrate that RepRap components have mechanical properties comparable to those produced using commercial 3D printing. Results show that the average tensile strength of PLA and ABS are 56.6 MPa and 28.5 MPa, respectively, and the elastic modulus are 3368 MPa and 1807 MPa, respectively. Inexpensive open-source 3D printers can

be considered mechanically functional as those from commercial vendors. However, configuration, operation, and turning details of each printer, including its type, age, and calibre of the employed polymer filament, need to be taken into account.

Caminero *et al*. [12] studied the performance characteristics of PLA samples with various process parameters. This study describes how feed rate, layer thickness, and print alignment affect the performance characteristics of PLA samples made using a low-cost 3D printer. Anisotropic behaviour can be observed in the experiment as 3D printing is done layer by layer. To determine the mechanical properties of printed parts, a 3-point bending test and a tensile test are conducted. This work focuses on upright, flat, and one-edge configurations of PLA samples. The upright orientation shows the lowest mechanical properties, while the flat and one-edge configurations have the best strength and stiffness. Ductility declines as layer thickness and feed rate increase. As layer thickness rises and maximum feed rate decreases, mechanical characteristics differ to maintain the upright position.

Alafaghani andQattawi [13] investigated the influence of process parameters on FDM parts. This work is centered around the different variables, also known as 3D printing parameters, used in the FDM technique. These variables include the extrusion temperature, infill pattern, layer thickness, and infill percentage, which are the focus of Taguchi's DOE research. The precision of the dimensions and mechanical characteristics of the FDM segments are indicators of the effect of the processing parameter. To achieve higher dimensional precision, a hexagonal infill pattern, lower infill percentage, thinner layers, and lower extrusion temperature are necessary. However, the current FDM production method often results in components that are larger than the CAD model. To strengthen FDM, a higher extrusion temperature, triangular infill pattern, ideal layer thickness, and larger infill percentage are required. Additionally, ductility can be improved by thickening the layers and using a rectilinear infill scheme.

Yao *et al.* [14] utilized the ISO 527-2-2012 standard to create 3D printed specimens with differing printing angles (0°, 15°, 30°, 45°, 60°, 75°, 90°) and layer thicknesses (0.1mm, 0.2mm, 0.3mm) for each angle. The study investigated the final tensile strength of FDM PLA materials, as well as the mechanical analysis and design of 3D printed components, from various printing perspectives. To predict the ultimate tensile strength of FDM with PLA materials, the researchers developed a theoretical transversal isotropic hypothesis-based model, the traditional theory of lamination, and the Hill-Tsai anisotropic yield standard. These concepts are confirmed through tensile tests, which showed that a lower printing angle

and thicker layers resulted in lower tensile strength. The calculation findings are more consistent with the model developed than with previous models, as it included two distinct in-plane shear modulus calculation methods.

Alafaghani *et al.* [15] conducted an experimental analysis to investigate the impact of each processing parameter on the mechanical properties of the FDM parts and dimensional accuracy. The study observed the effects of infill percentage, infill pattern, print speed, building direction, layer height, and extrusion temperature on the mechanical properties and dimensional accuracy. The study also presented an FEA model for AM parts. The results showed that layer height, building direction, and extrusion temperature have a greater impact on the dimensional accuracy and the mechanical properties than infill pattern. The research proposes modeling their behavior under mechanical loads to more thoroughly examine the combined effects of processing parameter modifications.

Raj *et al.* [16] investigated on biodegradability and strength of Poly Lactic Acid. Environment friendly design, cost effectiveness and production time of a production process plays an important role in industry 4.0. In a study Poly Lactic Acid (PLA) was found to be a viable alternative to current materials due to its biodegradability and strength, two essential qualities for manufacturing newer components using 3D printing. To test the material's strength and biodegradability, a solid 3D model was chosen based on ASTM standards and subjected to micro tensile testing and landfill testing. The results showed a weight reduction of 6.22% after a four-week landfill test, indicating that PLA can be used as a biomedical component. However, it is important to note that PLA's mechanical properties may change over time due to environmental factors, which is a disadvantage for biomedical components.

Fernandez-Vicente *et al.* [17] worked the effect of infill density and infill patter on 3D printed parts. The way that honeycomb and rectilinear designs are constructed affects the deposition trajectories and bonding between layers. This study examined the impact of two controlled variables, infill density and pattern, on the strength of 3D printed components. Various test components are printed on an open-source 3D printer with different infill patterns and densities. The results showed that although the behavior was similar, the printing pattern had a small effect on maximum tensile strength, less than 5%.

Johnson and French [18] investigated the mechanical properties of filaments intended on polymer. While consumer-level 3D printers have improved in the past decade, this study aimed to fill the information gap regarding the mechanical properties of filaments intended

for consumer use. The study tested commercially available filaments made of different materials, including PLA, ABS, PETG, various nylons, Polycarbonate/ABS, and ASA, at different infill rates.

Naik *et al.* [19] conducted a study on the tensile characteristics of Multi-Infill Pattern (MIP) specimens made using Fused Deposition Modeling (FDM) based on printing orientation. Poly-lactic acid (PLA) is chosen as the source material, and the thermal stability of PLA is assessed using Thermal Gravimetric Analysis (TGA). The study focused on flat and on-edge print orientations due to their impact on the strength of the parts. The MIP is made up of different designs with various infill densities. The results showed that printing orientation had an impact on the tensile strength of the specimens, with the on-edge orientation providing the highest strength. Compared to specimens with a single infill pattern, MIP specimens had greater tensile strength. The study also showed that modifying the density of models created using the FDM process is possible using an air gap or infill parameter. The experiment used PLA specimens and examined the impact of layer thickness, deposition angle, and infill on the maximum flexural force.

Lužanin *et al.* [20] worked on experimental analysis of the influence in FDM specimensmade of PLA. A 2^3-factorial experiment is conducted with three centres, but without replication on. The results indicate that extrusion speed has a dominant and statistically significant impact, and that there is a significant interaction between deposition infill and angle, with nonlinear effects.

Pernet *et al.* [21] investigated the mechanical behaviours, environmental and economic advantages of different infill patterns. In order to reduce the weight of 3D printed products, various infill patterns have been used to reduce material usage. However, designers and engineers often struggle to choose the most appropriate infill structure, which can result in missed opportunities for cost and material productivity improvements. This study aims to investigate the mechanical behaviours, environmental and economic advantages of different infill patterns, using compression tests and life cycle cost estimates. Fourteen common infill patterns, including grid, lines, triangle, cubic, tetrahedral concentric 3D, concentric, zigzag, Gyroid, octet, cross, cross 3D, quarter cubic, and trihexagonal are analysed. The study found alternative design options for infill patterns in additive manufacturing.

Lee *et al.* [22] worked the use of shell-infill structures in additive manufacturing (AM) through a systematic design process. Multi-scale topology optimization is employed on the

basis of the homogeneity design technique to create a structure with a coated surface and an orthotropic inside that varies spatially. The proposed method involves five steps, which include techniques for homogenization, topology optimization, and de-homogenization. The homogenization process generates the net elasticity tensor of the orthotropic infill microstructure in accordance with the microstructure design parameters. The topology optimization stage creates both the infill microstructure and coated macrostructures simultaneously by optimizing the microstructure design variables and density design variable. The de-homogenization process restores a spatially varying infill microstructure. This method can be applied to a range of physical problems, such as thermal and electromagnetic issues. In terms of design flexibility, heterogeneous anisotropic infill structures are preferred to homogeneous isotropic structures.

Jain and Gupta [23] have investigated the impact of FDM processing parameters on printed complex lattice structure. PLA Lattices have numerous applications, including in the automotive, aircraft, smart textiles, bio-printing, shape-resuming memory components, and medical implants industries. To create an effective PLA lattice, various parameters such as unit cell forms, volume fragment, and size must be considered. The commonly used BCC, octet truss, and CCP unit cells tend to fail due to stress build-up at the truss joining edges. Therefore, the current study has developed a strong CCP lattice structure by optimizing design elements such as unit cell and lattice size, layer height, support kinds, filament print temperature and speed, infill density and pattern, build orientation and temperature, and other influencing factors to enhance the 3D printed lattice part's strength.

Ambati and Ambatipudi [24] have examined the effect of infill pattern and density on the mechanical properties of PLA. The truss lattice, which is structured like an octet, is recommended for load-bearing applications because it can handle heavier loads. However, designing it can be challenging. The mechanical properties of PLA, a material used in 3D printing, are affected by various factors such as infill design and density. To evaluate the mechanical attributes like tensile strength, PLA parts printed with three different infill patterns (grid, gyroid, and triangle) and infill densities (60%, 75%, and 90%) are examined. The best parametric conditions are identified. The grid pattern is found to offer superior resistance as the filler material is aligned with the tensile stresses being applied, unlike the other two designs. Increasing infill density in 3D printed specimens improves tensile strength.

Mishra *et al.* [25] conducted a study on the impact of process parameters on the mechanical properties of 3D-printed products. The minimization of waste, design, fast prototyping, and manufacturing of complex shapes make additive manufacturing a revolution for industry 4.0, as stated in this article. The purpose of this review is to provide a brief overview of additive manufacturing processes, with a particular focus on the Fused Deposition Method (FDM) and its processing conditions, such as infill pattern and infill density, and their effects on the physical behaviour of 3D printed components.

Guajardo-Trevino *et al.* [26] research focuses on how additive manufacturing process conditions affect part strength, and how path planning and design attributes can induce flaws. The research discusses the use of quick prototyping in practical and business settings. This article aims to clarify how density and infill patterns affect the physical characteristics of printed objects for both academic and commercial purposes. Production characteristics such as raster angle, raster gap, number of contours, and raster width have a positive impact on strength but cannot be controlled directly. The study investigates the effect of internal voids and raster gaps on the compressive strength of composites using compressive testing and computer simulations. Non-linear simulations of voids and gaps in geometries offer a good description of the behavior of the part consistent with experimental results.

Wang *et al.* [27] conducted research on the physical properties of these structures, exploring factors such as strain rate, unit pattern, and infill density. The infill pattern is found to be a predictable cause of deformation and failure types in 3D printed structures, mainly due to printing errors. Their goal is to understand how infill parameters and tensile strain rate affect the elastoplastic deformation and failure behaviours of polyamide-based composite structures produced by FDM technology. The research included examining the mechanical characteristics and relative energy absorption of composite structures, with a focus on the effects of infill pattern, infill density, and tensile strain rate. The study found that higher infill densities resulted in more flaws and decreased elongation at break in composite constructions, while increased infill densities are associated with higher young's modulus. The research also included capturing morphological evolution concurrent with the mechanical research.

Srinidhi *et al.* [28] conducted an examination of various infill patterns, including grid, honeycomb, rectilinear, and cubic, on components made of polyethene terephthalate glycol (PETG) and carbon fiber-strengthened polyethene terephthalate glycol (CFPETG) to measure their hardness, tensile effect, and flexural strengths. Their secondary goal was to enhance the

interlayer bonding of printed samples through post-processing annealing. The results showed that the annealed PETG and CFPETG grid pattern had the greatest increase in stiffness, tensile strength, impact strength, and flexural strength.

Ali *et al.* [29] investigated the mechanical properties onFDM based printed components made of Polyamide 6 (PA6) and polyamide 66 (PA66). Polyamides 6 (PA6) and 66 (PA66) were compared to examine their mechanical qualities for cost-effective and efficient component creation. The ultimate tensile strength of rectilinear buildings based on PA6 with a 100% infill percentage was the greatest, while the UTS of printed samples increased with an increase in infill percentage.

Abbas *et al.* [30] (PLA) focused on the impact of infill density on the compressive strength of FDM specimens made of polylactic acid. The results of the experiment indicate that lower infill values lead to faster building speed, higher infill values result in longer printing time, and increasing infill densities enhance the compressive strength of 3D-printed PLA samples. The study used compression tests to determine the effect of infill percentage on compressive strength and found that solids had the highest compressive strength. It is also discovered that compressive strength and infill percentage have a roughly linear relationship.

Sandhu *et al.* [31] used Taguchi-designed L9 orthogonal array (OA) method to investigate the impact of various fused deposition modelling (FDM) process variables on multiple mechanical properties, such as young's modulus and surface roughness, of FDM prints (DOEs). The specimens are composed of PLA, and the key input parameters are the infill pattern, raster angle, and layer thickness. The highest strength and elongation values are 38.91 MPa and 6%, respectively, while the average surface roughness ranged from 4.44 μm to 7.18 μm, with 3.18 μm to 9.21 μm in the x axis and 3.133 m to 9.512 m in the y axis. When using a layer thickness of 0.16 mm, a cubic infill pattern, and a raster angle of 60, specimens exhibited excellent mechanical properties.

Kumar and Ranjan [32] focused on the elongation property of nylon-6 thermoplastic prototypes made using fused filament fabrication (FFF) technology. The FFF process is carried out by changing input factors such as infill percentage, bed temperature, and outer perimeters. The study used the signal to noise ratio of the elongation property to optimize the elongation properties. According to the research, the ideal conditions for FFF technique include a higher infill percentage (100%) and an intermediate bed temperature (60°C), as they allow the part to maintain its maximum elongation. This information is derived from altering

the infill percentage (70, 85, and 100%), bed temperature (50, 60, and 70°C), and outer perimeters (4, 5, and 6).

Dharmalingam *et al*. [33] worked on different infill rates of PLA components. PLA, a natural product made from corn, cassava, and sugarcane, is a renewable and environmentally friendly resource that plays a crucial role in the manufacturing industry. However, it is found that PLA produced using the FDM method had lower impact strength than PLA produced using injection moulding. To overcome this drawback, researchers turned to PLA due to its biodegradable and eco-friendly nature. Through experiments, it is discovered that PLA deposited using FDM had higher impact strength than IM. Using FEA based ANSYS software, it is assessed the impact strength of PLA at various infill rates and found that printing with on-edge orientation in the width direction resulted in a higher impact strength than IM samples.

Gunasekaran *et al.* [34] studied the effect of infill percentage on the physical characteristics. They used wire filament made of PLA and constructed specimens using the FDM technique with varying infill densities. The infill density of PLA-printed samples is altered to 25%, 50%, 75%, and 100%. The study revealed that specimens printed with 100% infill density had better mechanical properties. Furthermore, as infill density increased, the mechanical properties of the printed specimens also improved. The mechanical testing of printed specimens is carried out according to ASTM standards, which included measurements of hardness, tensile, impact, and flexural strength. For the specimens printed with 100% infill density, the corresponding values for hardness, tensile strength, impact strength, and flexural strength are 97 HRC, 53 MPa, 70 J/m2, and 53 MPa, respectively.

Sukindar *et al.* [35], focused specifically on the effect of process parameters on the tensile strength of polylactic acid (PLA) materials. The use of rapid prototyping technology allows for a high degree of control over the variables involved in the fabrication process, as noted in the study. By adjusting factors such as layer thickness, shell thickness, and printing speed, the researchers are able to print samples using open-source 3D printers and Repetier-Host software. Analysis of the results of tensile testing using ANOVA showed that the thickness of the shell had a significant impact on tensile strength. It is important to note that the mechanical properties of printed objects are indirectly influenced by layer thickness.

Luo *et al.* [36] studied the optimal approach for constructing buildings involves filling confined gaps or voids in foundation structures with a lighter, porous infill material. The

authors provide a method for calculating this automatically and optimizing the arrangement of these spaces using infill. This involves using a nonlinear virtualized temperature filter to distinguish between closed and open areas, and combining it with a PDE filter and projection method to create a special interpolation for structures with infill-supported voids. This method can also be applied to structures without enclosed voids. Additionally, the authors use the resilient topology optimization formulation and the adjoint method to generate vulnerability equations.

Claver *et al.* [37] investigated the effects of layer height, infill density, and layer orientation on the mechanical performance of test samples made of PLA and ABS. The responses under investigation include tensile yield stress, tensile strength, nominal strain at break, and modulus of elasticity. The infill % is the production parameter that has the greatest impact on the outcomes, especially in PLA. ABS is less unpredictable compared to PLA. PLA is a strong candidate for additive manufacturing due to its strong connection between layers and superior tensile strength and stiffness in comparison to ABS. These findings are supported by various sources.

Travieso-Rodriguez *et al.* [38] worked on the mechanical properties of polylactic acid (PLA) pieces made through fused filament manufacturing behaved under different production parameters. The researchers used an L27 Taguchi experimental array to study the flexural resistance of PLA specimens, considering six parameters: layer height, filament width, fill density, layer orientation, printing velocity, and infill pattern. They used a four-point bending machine and a rotating bending machine to test different geometries and discovered that layer orientation is the most significant factor, followed by layer height, filament width, and printing velocity. Fill density and infill pattern didn't seem to have any noticeable effect.

Suteja *et al.* [39] conducted research to examine how different 3D printing parameters affect the mechanical properties of PLA items, with a focus on the importance of infill design parameters such as layer thickness, infill pattern, infill density, infill width, and infill deposition speed. This study found that these parameters have a significant impact on the mechanical properties of 3D-printed items, with layer thickness affecting tensile and yield strengths and infill deposition speed decreasing them. Additionally, infill density and layer width affect compression and flexural strength, while larger infill densities increase stiffness and elastic modulus. Finally, an increase in layer thickness leads to an increase in ductility.

Pucklitzsch *et al.* [40] examined the infill construction made of hollow spheres packed in a closed hexagonal pattern and simulated the intersection created by the contact between the spheres. There is a lack of research on the mechanical properties of constructions that have regularly arranged hollow spheres, possibly because creating these structures is more challenging than irregular ones like foams. As a result, little is known about how well they function mechanically. However, with the help of additive manufacturing, hexagonally packed cylindrical samples filled with hollow spheres are created for study. The cylinder's internal structure is designed using a script-based technique, and the Finite Element Method is used to investigate the deformation behaviour. Compression tests on cylindrical specimens produced through additive manufacturing validated the results. The study found that proper modelling of the contact between the spheres improves structure stability, mechanical properties increase with increasing density, and reducing the relative spherical wall thickness increases ductility.

Farbman *et al.* [41] conducted an experiment that examined how various factors affect the mechanical characteristics of 3D-printed materials. In accordance with ASTM guidelines, the team conducted a series of monotonic tensile tests on 3D-printed plastics. A total of 13 "dog bone" test specimens were used in the experiment, with alterations made to the material, infill percentage, infill geometry, load direction, and strain rate. The researchers carried out comparative analysis on the strength-to-weight ratios of different infill geometries. The results showed that as the infill percentage decreased, the specific ultimate tensile strength (MPa/g) also decreased. Additionally, the hexagonal infill pattern was found to be stiffer and stronger than the rectilinear pattern. Fused deposition modelling (FDM) is one of the most commonly used additive manufacturing (AM) techniques for creating polymer components with simple to complex geometries.

Patil *et al*. [42] worked on a multi-objective optimization approach to optimize the process parameters for FDM (3D printing) of PLA components. The experiment utilized various parameters such as infill patterns, infill percentage, printing speed, and layer thickness, while the analysis is based on surface roughness, printing duration, and filament length used. The ideal settings for this experiment are determined to be triangle patterns, 70% infill, a printing speed of 100 mm/h, and a layer thickness of 0.2 mm. The results obtained from these optimum parameters showed a surface roughness of 12.560 m, a printing time of 88 min, and a filament length of 4.22 m. Implementing the GRA optimization paradigm resulted in a

10.10% improvement in GRG over the initial parameter settings. Regarding the parameters studied, it is found that printing speed had the least impact on FDM performance.

Bachhav and Sonawwanay [43] studied the effect of infill pattern on mechanical properties of PLA components. Previously, additive manufacturing research mainly focused on modifying factors such as air gap, line width, printing speed, extrusion material and temperature. However, there has been very little research on infill patterns and percentages, with only experiments being conducted. Research on infill patterns is important as it can impact product quality, material and production costs. Most studies have been based on experiments using different single process parameters. In this study, simulations are conducted on triangular and rectangular patterns with 50% and 70% infill. Results showed that the triangle pattern generates more stress at 50% infill, while the rectangular pattern generates more stress at 70% infill. Therefore, triangular patterns are better suited for 50% infill applications, while rectangular patterns are better suited for 70% infill applications. The study also analyzed the geometrical features of commonly used infill patterns for filling 3D-printed items by implementing various patterns in a generic cube slicing process to calculate the lowest density error.

Majd *et al.* [44] studied the accuracy of infill density in metal additive manufacturing processes by examining commonly used 2D infill patterns and their input parameters. They found that infill density accuracy is especially important in metal additive manufacturing. Previous research has primarily focused on printing factors and strength as an output response, but little has been done on cellular geometry and nozzle diameter or combinations of output responses.

John *et al.* [45] investigated various process parameters effect on printed components using DOE and Grey Relational Analysis. The study fills this gap by focusing on cell geometry, nozzle diameter, and strain rate using the Taguchi design of experimentation and Grey Relational Analysis. The results show that 0.8mm nozzle diameter, 5mm per minute strain rate, and square cellular shape produce the best grey relational grade.

Yadav *et al*. [46] conducted a study on the mechanical characteristics of FDM-printed objects, focusing on the effects of extrusion temperature, infill density, and material density. The investigation revealed that both extrusion temperature and infill density had an equal impact on tensile strength. This article discusses the tensile strengths of ABS, PETG, and multi-material test pieces, as well as the effects of material density, infill density, and

extrusion temperature. Multi-material objects are created by layering 50% ABS and 50% PETG using FDM 3D printing, using ASTM Type IV. In order to improve the mechanical properties of FDM-produced objects, infill density and extrusion temperature are optimized using MATLAB 16.0 and the ANN and GA-ANN hybrid tools. Empirical verification showed that the GA-ANN method increased tensile strength by up to 4.54%.

Doshi *et al*. [47] conducted a thorough examination of the FDM process and concluded that adjusting printing settings can significantly improve both the tensile strength and Young's modulus independently and simultaneously. Several studies have used the concept of the desire function to approximate optimum factor levels for real-time optimization, which involves various ideal factor settings. ABS, PLA, and nylon are the most popular materials for FDM printing due to their wide availability and ease of machinability. Young's modulus performance of 3D printed material is found to be best at an infill speed of 90 mm/s, with the layer structure also being the best at this rate, resulting in the lowest level of porosity. The ideal printing temperature for Polyester resin is found to be 215. However, it is challenging to identify the specific causes of the relationships between different elements and characteristics, and how different limitations interact with each other. Despite this, the FDM part-built mechanism remains a complex phenomenon.

2.4 Motivation of Present work

Manufacturing companies have been focusing on increasing accuracy and reducing production time, costs, material waste, and required assembly pieces since the industrial revolution, also known as industry 4.0. Engineers work towards developing more error-free methods for complex part manufacturing at lower costs. To meet demand, advanced manufacturing technologies like AM have been adopted, with FDM being a popular and affordable polymer-based process. Polymers are preferred due to their strength, lightweight, corrosion resistance, environmental stability, and lower cost. FDM printing technology utilizes polymers such as PLA, ABS, PC and polymer composites. PLA is a promising thermoplastic aliphatic polyester with complete biodegradability, good optical qualities, processing capabilities and reasonably high mechanical strength. The goal is to create an ASTM D 638 Type IV standard PLA specimen using FDM technology and determine its mechanical properties for industrial applications. This inspiration is derived from the knowledge mentioned above.

2.5 Objective of Present Work

After examining various literature, the objective of the present research has been established. The aim is to investigate how process parameters, such as overlapping percentage and raster angle, affect the ultimate tensile strength (UTS) of PLA.

CHAPTER III

EXPERIMENTAL INVESTIGATION of 3D PRINTED PLA by FDM

3.1 Experimental Investigations

The main goal of using Fused Filament Fabrication (FFF) for polymeric elastomers is to create and manufacture functional components that have improved mechanical properties. FFF provides significant benefits in producing these parts with various structures. ASTM D638 refers to different types of test specimens depending on the material being tested, the thickness of the material, and the features observed when it breaks. A commonly used method for determining the tensile strength of reinforced and unreinforced plastics is the ASTM D638 test, which involves using a traditional dumbbell or dog-bone-shaped sample with consistent temperature, humidity, and test speed. This method allows for examining materials up to 14 mm thick.

The rectangular ASTM D3039 test specimen consistently met the specified failure acceptance criteria of the standard. In comparison to ASTM D638 geometries, rectangular ASTM D3039 samples have a higher elastic modulus and a lower ultimate tensile strength. According to ASTM D638, the Type I specimen is suitable for evaluating reinforced composite materials. However, the results of this study consistently showed that the rectangular ASTM D3039 test specimen provided reliable test results across a set sample size. If the thickness of the samples exceeds 14 mm, they should be cut down to the correct thickness. When testing materials less than 1 mm thick, the preferred test technique is ASTM D882. The Type I specimen should be used when there is enough material that is 7 mm thick or less. If the selected Type I specimen does not cause the material to break in the narrow section, it is recommended to use a Type II specimen. For materials with a thickness greater than or equal to 7 mm but not exceeding 14 mm, a Type III specimen must be used. When comparing materials of different stiffness, Type IV specimens are typically employed. For this experimental work, a Type IV specimen with a thickness of 4.0 mm according to ASTM D 638 has been chosen as shown in Figure 3.1.

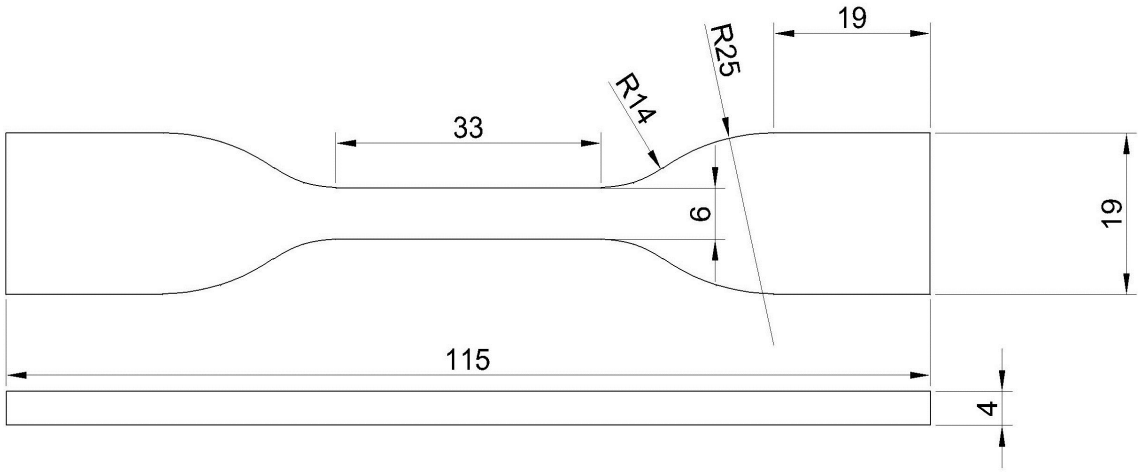

Fig. 3.1 ASTM D 638 Type IV Specimen

The sample is in the shape of a dog bone and has a narrower section in the middle called the gauge section. The cross-sectional area of the gauge section is smaller than the ends of the sample. This design ensures that the sample will fail within the gauge section during the tensile test. The narrow section has a width of 6 mm and a length of 33 mm. The overall length of the sample is 115 mm and the overall width is 19 mm. The gauge length is 25 mm and the distance between the grips is 65 mm. The fillet has a radius of 14 mm and the outer radius is 25 mm. The thickness of the sample is 4 mm.

The foundation of FDM technology involves extruding and depositing molten material onto a printing plate in a layer-by-layer manner. PLA and ABS are the most commonly used filaments for this process, but other specialized thermoplastics like PETG, ASA, Nylon, Ultem, etc. can also be utilized. There are essentially four types of FDM 3D printers: Cartesian, Delta, Polar, and those utilizing robotic arms. 3D printing is a significant form of additive manufacturing, where materials are added layer by layer to create models, prototypes, or products. This process is also known as Fused Filament Fabrication, Fused Deposition Modeling, or Filament Freeform Fabrication. Although time-consuming, it enhances the mechanical properties of the products. Understanding how different parameter values in the 3D printing process influence the mechanical characteristics of the item is crucial.

Due to its lower density and greater strain at failure, polymer is commonly used as a material for prototypes. Moreover, polymers are stronger than metals when compared by weight. Polylactic acid (PLA) is a popular polymer for 3D printing due to its low melting point and energy-efficient printing process. PLA is also biodegradable, emitting no odors or harmful vapors. Additionally, it does not require a heated base and adheres well to the platform. Therefore, PLA is the chosen material for this research. The findings from this study will provide insight into the factors that affect the mechanical properties of PLA parts. To achieve this objective, the research will first review previous studies on PLA 3D printing techniques. It will then identify key process variables and their impact on the mechanical properties of 3D printed objects.

Certain techniques involve melting or softening the material to form layers. Fused filament manufacturing, also known as fused deposition modelling (FDM), is a process where a model or part is created by extruding small beads or streams of material that quickly harden into layers. A thermoplastic, metal, or other material filament is fed into the extrusion nozzle head of a 3D printer, which heats and controls the flow of the material. The range of shapes that can be made with FDM is limited. Another method involves melting parts of the layer, moving up in the working area, adding another layer of granules, and repeating the process until the item is complete. This method eliminates the need for temporary supports by using the unfused material to support overhangs and thin walls in the part being made. To avoid converting to filament, FFF/FDM now allows for 3D printing directly from pellets. This process, known as fused particle fabrication (FPF) or fused granular fabrication (FGF), allows for the use of more recycled materials. Additive manufacturing, or 3D printing, has become increasingly important in the technical world due to its many advantages. These advantages include increased product customization, reduced manufacturing costs, faster prototyping, and improved product quality. The possibilities of 3D printing have also been applied in renewable energy systems. 3D printing technology can be used to create battery energy storage devices, which are essential for the generation and distribution of renewable energy. Another advantage of 3D printing is its ability to accurately manufacture complex geometries. This is particularly useful in the field of microwave engineering, where 3D printing can be used to create parts with unique qualities that are difficult to achieve with traditional manufacturing processes.

3.2 Equipment

3.2.1 FDM 3D printers Creator Pro 2

The FDM 3-D printer depicted in Figure 3.2 is utilized to create the specimens. The Creator Pro 2 is an upgraded version of the original creator series. With its independent dual extruder system, the Flashforge Creator Pro 2 offers beginners improved quality and easier operation. It effectively solves the issue of stringing that a traditional independent twin extruder 3D printer is prone to. The print volume of the Creator Pro 2 is 200 mm ×148 mm ×150 mm. The key features of the Creator Pro 2 include an independent dual extruder system and a classical structure. The independent twin extruder system allows for the simultaneous printing of two identical pieces, doubling the printer's output speed and making it more suitable for serial production. By printing two identical models with mirror images of each other, productivity is doubled. Printing a complex structure on soluble support enables the production of better printed objects. The Creator Pro 2 is capable of printing a single object using two different materials. To ensure reliable printing, the Creator Pro 2 maintains a metal frame structure. The enclosed print chamber reduces the impact of the surrounding environment on printing. These improvements enhance the printer's ability to work with various filaments. It supports PLA, Pearl PLA, ABS, ABS Pro, PVA, and HIPS. The FDM 3-D printer has a touch screen interface as shown in Figure 3.3. The FlashPrint software generates the G-code for the 3D printer. The specifications of the Creator Pro 2 and details of the software are listed in Table 3.1 and 3.2.

Fig. 3.2 FDM 3-D printer Creator Pro 2

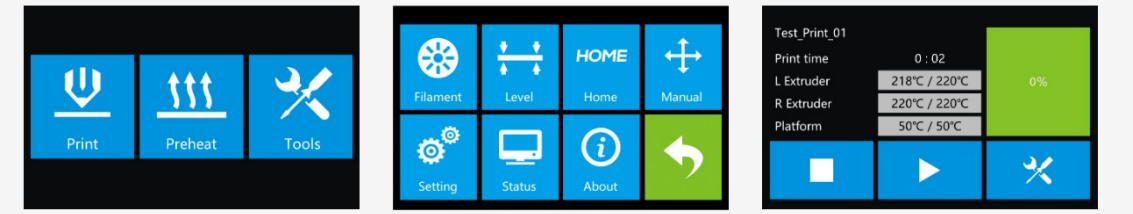

Fig. 3.3 Touchscreen interface

Table 3.1 Specification of Creator Pro 2

Parameters	**Values**
Extruder Quantity	2
Nozzle Diameter	0.4 mm
Maximum Extruder Temperature	240 °C
Print Speed	30 – 100 mm/s
Maximum Platform Temperature	120 °C
Filament Compatibility	PLA, ABS, PVA, HIPS
Filament Diameter	1.75mm (0.069IN)
Print Volume	200 mm ×148mm ×150 mm
Layer Thickness	0.10 to 0.40 mm
Print Precision	± 0.2 mm

Table 3.2 Details of the Software

Software	FlashPrint
File Input Format	STL/3MF/OBJ/BMP/JPG/JPEG/FPP/PNG
File Output Format	X3G files

3.2.2 Material Properties of PLA

In this study, PLA polymer is used. Polylactic acid (PLA) is a type of thermoplastic polyester that is both biodegradable and bioactive. It is derived from renewable resources like corn starch or sugarcane, making it a sustainable option compared to conventional plastics made from petroleum. The characteristics and properties of PLA are detailed in Table 3.3.

Table 3.3 Characteristics and properties of PLA

Property	**Values**
Density	1250 Kg/m 3
Specific Heat	1800 J/(kg·K)
Melting Point	115-230 ºC
Tensile Strength	35.60 MPa
Thermal Conductivity	0.13 W/m.K
Glass Transition Temperature	60ºC
Flexural Strength	80 MPa
Impact Strength (Unnotched) IZOD	96.1 (J/m)
Shrink Rate	0.37-0.41% (0.0037-0.0041 in/in)

3.2.3 UTM

Instron® offers a variety of high force universal testing machines that can conduct mechanical tests on materials and products, such as tensile, compression, bend, peel, tear, and more. These machines are designed to meet industry standards like ASTM and ISO. Instron provides systems in different sizes and with varying maximum force capacities to cater to different applications. From automotive sheet metal to reinforced bar, pipe, and tubing, Instron's high force testing systems are well-suited for various metals testing requirements. Instron systems are designed to adapt and grow alongside the changing needs of industries, providing a comprehensive solution for tension, impact, fatigue, bend/flex, shear, and torsion testing.

Instron provides a variety of grips and adapters that can meet strict alignment standards. These accessories enable you to conduct tension and/or compression tests without having to remove the main grips and affecting the alignment of the system. They are also compatible with chambers for testing in non-standard environments and advanced extensometer for precise strain measurements. The tensile tests are carried out using the Instron 5582 Universal machine, with a capacity of 100 kN as shown in Figure 3.4.

Fig. 3.4 Instron 5582 tensile testing machine

Test Fixtures:

- Wedge Grips for tension testing with a variety of faces
- Platens for evaluating compression
- Flexure testing setup with three points

Machine Highlight:

- Capacity of the machine is up to 100 KN.
- Operating speed is 0.05 to 500mm/min.
- Operating temperature up to 300 C
- Metals and their alloys, wide range of polymers and ceramics are workable materials.

- Tension, Compression and Bend test can be done.
- Bluehill Universal software has been used to operate the machine as well as to analyze data.

3.3 Methodology

The present experiment involves three main steps: preparing a 3D CAD model, creating specimens, and conducting a tensile test. Thermoplastic PLA is particularly user-friendly and offers greater stiffness and strength compared to nylon and ABS. PLA is also one of the easiest materials to successfully 3D prints due to its low melting point and minimal warping. Consequently, polylactic acid (PLA) has been chosen as the focus of this experiment due to its widespread use as a 3D printing material. The steps involved in the FDM process are illustrated in Figure 3.5.

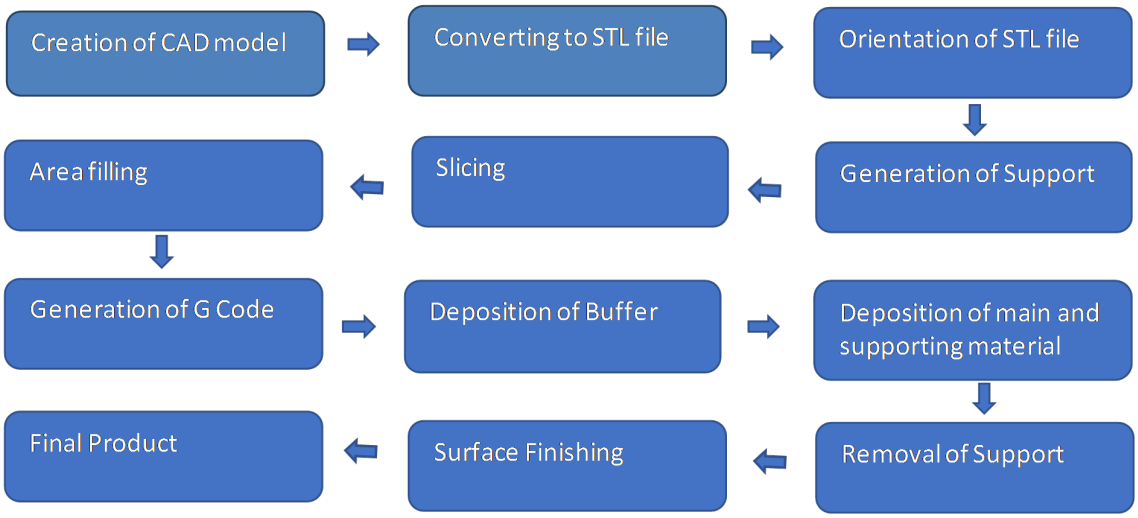

Fig. 3.5 Sequences of the FDM Process

The mechanical properties of 3D printed products can be improved by considering various factors during the printing process. These factors include nozzle size, filament size, melting temperature, bed heat, printing speed, layer thickness, infill density, number of layers, raster angle, raster gap, and raster width. For this experiment, two specific process parameters are chosen: raster angle and path width. The first step in producing a sample is creating a CAD 3D model in STL format, which must meet the requirements stated in the ASTM D 638 Type 4 standard. The "flashPrint" software is used to create samples before printing, and it utilizes

the STL file to specify settings and generate G-code for 3D printing. The Creator Pro 2 FDM 3D printer is then used to print the samples. The samples are printed flat by depositing multiple layers of 1.75 mm diameter PLA green filament until the desired thickness is achieved. The flat position is chosen to better understand the effects of printing direction, although it may result in inferior mechanical properties compared to the on-edge position. Throughout the experiment, certain factors are kept constant, such as a printing surface temperature of 210°C and a bed temperature of 30°C. The printing is done at a speed of 20 mm/s with a nozzle diameter of 0.4 mm. The specific printing process parameters used in this experiment can be found in Table 3.4. The printer during the sample preparation is depicted in Figure 3.6.

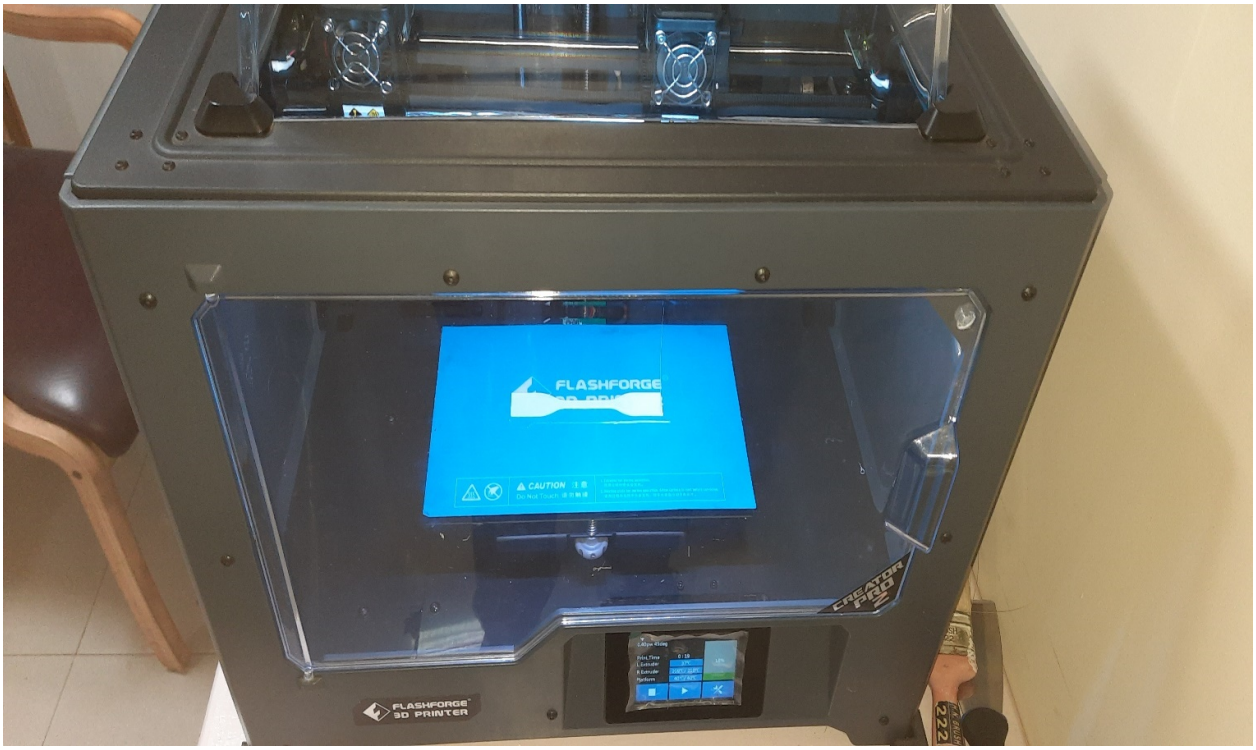

Fig. 3.6 Creator Pro 2 printer duringthesamplepreparation

Table 3.4 The printing process parameters for test specimens

Printing parameters	**Values**
Platform Temperature	30 °C
Base Print Speed	20 mm/s
Travel Speed	20 mm/s
Slice Profile	Fine
Shell Count	1
Fill Density	100%
Fill Pattern	Line
Raster Angle	90°, 45°, 0°
Path Width (mm)	0.40,0.38,0.36,0.34,0.32,0.30,0.28
Path Precession	0.20

The printing process occurs at a bed temperature of 30 °C and a nozzle temperature of 210 °C. The nozzle's printing speed is 40mm/s and its diameter is 0.40 mm. This means that the material extracted from the nozzle is also 0.40 mm. Once the process begins, we cannot change the nozzle diameter, but we can adjust the pitch by altering the path width. This results in the overlapping of the extracted layers. For this experimental work, we took a total of 21 samples using seven different path widths and three different raster angles. The path width decreases from 0.40 mm to 0.28 mm, while the percentage of overlapping increases from 0% to 30%. This overlapping leads to stronger bonding of the specimens compared to specimens without any overlap. While there has been extensive research on other process parameters, very little has been done regarding path width. Therefore, we chose to focus on path width and raster angle for our specimen printing.

CHAPTER IV
RESULTS AND DISCUSSION

4.1 Introduction

Fused Deposition Modeling (FDM) is a widely utilized additive manufacturing (AM) technology that falls under the category of material extrusion processes. In FDM, molten material is extruded from a nozzle and deposited layer by layer to create a three-dimensional object. PLA specimens are built using Creator Pro 2 3D printerfor tensile testing. The corresponding nozzle diameter is 0.40 mm. Printing process parameters such as overlapping percentage (0 %, 15 %, 30 %) and raster angles (0°, 45°, and 90°) are chosen. Tensile test is conducted using Instron 5582 Universal tester to evaluate the mechanical properties like Young's modulus, Yield Strength, Tensile Strength and Breaking Strength of the specimens.

4.2 Tensile Test

One of the most common tests used for evaluating mechanical properties of materials is the tensile test. In its simplest form, a tensile test is carried out by holding opposite ends of the element under test inside the load frame of the testing machine. The machine applies a tensile force, causing the test specimen to progressively elongate and eventually fail. Force-extension data, a quantitative measurement of how the specimen under test deforms under an applied tensile force, is typically monitored and recorded during this procedure. Tensile testing can quantify a number of important mechanical properties of a material by measuring the ratio of force to area. These mechanical characteristics found during tensile experiments include:

- Elastic deformation properties, such as the modulus of elasticity (Young's modulus)
- Yield strength and ultimate tensile strength,
- Ductility properties, such as elongation and reduction in area, and

Mathematically the Ultimate Tensile Strength can be written as,

$$\sigma = P_{max} / A_0 \qquad (4.1)$$

where, σ = UTS, P_{max} = Maximum Tensile Load, A_0 = Original cross section area.

Based on the stress-strain curve, the UTS value is a crucial mechanical property of a component because it illustrates the highest stress a material can withstand before failing. While designing a project, we can make decisions about when and how to employ a material by using the results of a UTS. The Bluehill universal software generates the curve for each analysedsample. The ASTM D638 type IVspecimen under tensile test in this study had a width, thickness, and gauge length of 6 mm, 4 mm, and 25 mm, respectively. The strain rate input is 0.00100 /s. The higher strain rate makes the material appear stiffer and stronger. A wide range of polymers, including plastics, and certain steels are sensitive to strain rate. At

higher strain rates, the properties of a material may not be accurately predicted from stress/strain data collected at lower strain rates. Fig. 4.1 (a-d) displays the specimens fabricated at different raster angles before and the specimens after testing.

(a)

(b)

(c)

(d)

Fig. 4.1 (a) 0°, (b) 45°, (c) 90° raster angle fabricated specimens, (d) specimens after tensile test

The raster angle, also known as the build orientation or layer orientation, refers to the angle at which successive layers are printed in processof 3D printing. The mechanical properties of the printed parts, including the UTS, can be influenced by the raster angle. The UTS measures the maximum stress a material can handle before breaking. The raster angle also plays a role in determining the direction of printed layers and affects the strength between

adjacent layers, known as interlayer adhesion. As raster angle increases 0° to 45° and then 90° the UTS value at 0% overlapping first increases then decreases.

When the raster angle changes, it changes the alignment of the printed layers in relation to the applied forces. UTS of the printed part can vary depending on the material properties and the raster angle. The impact of the raster angle on UTS can be attributed to factors such as anisotropy (different properties in different directions) and the strength of layer bonding. Additionally, the pattern of the raster will also affect the amount of material aligned at specific angles in relation to the loading direction, which in turn can affect its strength. It has been observed that the raster at 0° to the loading direction is the strongest, and then weakens as the angle increases up to 90°. At 0° raster angle and 0% overlap the UTS is 35.15 MPa at 45° raster angle and 0% overlap the UTS is 46.37 MPa and at 90° raster angle and 0% overlap the UTS is 38.32 MPa. At 0° raster angle and 15% overlap the UTS value is 40.68 MPa at 45° raster angle and 15% overlap the UTS is 39.93 MPa and at 90° raster angle and 15% overlap the UTS is 35.33 MPa. At 0° raster angle and 30% overlap the UTS value is 39.54 MPa at 45° raster angle and 30% overlap the UTS is 42.38 MPa and at 90° raster angle and 30% overlap the UTS value is 37.34 MPa. Here the UTS value first increases and then decreases or in a decreasing order as raster angle increases. It indicates different property in different directionand when the printing direction is changed equally the bonding area of two track wise extruded path also change.

The overlapping percentage, which is also referred to as the line width or extrusion width, pertains to the width of the individual lines or paths that are extruded by the 3D printer while printing. This width can affect the mechanical properties of 3D printed PLA (polylactic acid) parts, such as the ultimate tensile strength (UTS).

In the context of 3D printing, the overlapping percentage plays a role in the overall strength and structural integrity of the printed part. There are several factors to consider when examining how the path width affects the UTS. Firstly, the bonding between adjacent printed lines or layers is influenced by the path width. More overlapping percentage allows for more contact area and better adhesion between materials, resulting in improved interlayer bonding and potentially higher UTS up to a smooth extruded filament flow. Secondly, when adjacent paths overlap, it increases the contact area and promotes better bonding. A wider path width can increase overlap, leading to stronger interlayer bonding and improved UTS. Thirdly, PLA and other 3D printing materials may exhibit anisotropic behavior, meaning they may have different mechanical properties in different directions. The path width can affect the

anisotropy of the printed part, with wider paths potentially leading to increased UTS along the path direction. Finally, the path width also affects the amount of filament being extruded and deposited. A wider path requires more material, which can impact filament flow rate and cooling. It is important to properly control these parameters to ensure consistent material properties and layer bonding, ultimately affecting the UTS.

The mechanical properties of the fabricated samples are provided in Table 4.1, 4.2 and 4.3. Tensile tests are conducted at strain rates of 10^{-3} mm/s. At 0° raster angle and 15% overlapping, we obtain a maximum tensile strength of 40.68028 MPa when the load at UTS is 1.03830 kN and the yield stress is 14.55156 MPa. But Young's modulus of sample with 15 % overlappingis 2476.12 MPa which is higher compared to sample with 30% overlapping and less than sample with 0% overlapping. Flexibility is greater in a sample printed with a 0% overlapping than sample printed with a raster angle of 0°. For a path width of 0% overlapping and a raster angle of 45°, we obtain a maximum tensile strength of 46.37285 MPa when Young's modulus, load at the UTS, the yield strength and strain rate at the UTS are 1980.58 MPa, 1.24091 kN, 15.57464 MPa and 3.29354 with an extension at the UTS of 1.21104 mm. For 30% overlapping, we obtain a minimum tensile strength and at 30% overlapping, the maximum Young's modulus is observed for a 45° raster angle. The young's modulus, yield strength and load of UTS, UTS and UTS strain rate are 2576.89 MPa, 14.17537 MPa, 0.99566 kN, 42.38699 MPa, 4.45063%. In the case of raster angle of 90 degrees, we obtain maximum tensile stress at 0% overlapping. The Young's modulus, yield strength and load of the UTS, UTS, and the stress rate at the UTS of 0% overlapping width and 90° raster angle angle samples are 2196.40 MPa, 14.04149 MPa, 1.01596 kN, 38.32041 MPa, and 2.79588. In the case of a 90° raster angle sample, the minimum tensile strength is obtained at 15% overlapping.

In a total of nine experiments, the maximum tensile strength is obtained for an overlapping percentage of 0% with a raster angle of 45°, while the minimum tensile strength is observed on 0% overlapping with a raster angle of 0°. The maximum tensile strength of 46.37 MPa is observed at a raster angle of 45 degrees and an overlapping percentage of 0%. The minimum tensile strength of 35.16 MPa is observed at a raster angle of 0°and an overlapping percentage of 0%. The maximum breaking strength of 37.36 MPa is observed at a raster angle of 45° and an overlapping percentage of 30%. The minimum breaking strength of 20.64 MPa is observed at a raster angle of 45° and an overlapping percentage of 30%.

The maximum young's modulus of 2297.83 MPa is observed at a raster angle of 90° and an overlapping percentage of 15%. The minimum young's modulus of 1980.58 MPa is observed at a raster angle of 45° and an overlapping percentage of 0%.

Table 4.1 Tensile Test Result for Load and UTS

Sl. No.	Overlapping Percentage (%)	Raster Angle (Deg)	Youngs Modulus (MPa)	Load at Yield (KN)	Yield Stress (MPa)	Load at UTS (KN)	UTS (MPa)
1	0	0	2684.47	0.35036	13.18875	0.93397	35.15786
2	15	0	2476.12	0.37141	14.55156	1.03830	40.68028
3	30	0	2256.25	0.44916	17.15157	1.03547	39.54070
4	0	45	1980.58	0.42346	15.57464	1.24091	46.37285
5	15	45	2177.68	0.39428	14.63965	1.07558	39.93591
6	30	45	2576.89	0.36767	14.17537	0.99566	42.38699
7	0	90	2196.40	0.37227	14.04149	1.01596	38.32041
8	15	90	2297.83	0.31880	12.13988	0.92804	37.53993
9	30	90	2172.88	0.35112	12.98032	1.01022	37.34609

Table 4.2 Extension of Specimens during Tensile Test

Sl. No.	Overlapping Percentage (%)	Raster Angle (Deg)	Extension at Yield (mm)	Extension at UTS (mm)	Extension at Break (mm)
1	0	0	0.25129	0.85738	2.21795
2	15	0	0.27960	0.93870	0.97564
3	30	0	0.35214	0.94910	0.98121
4	0	45	0.34217	1.21104	2.01305
5	15	45	0.31472	1.06491	2.31104
6	30	45	0.28390	1.63650	3.43574
7	0	90	0.30814	1.01630	1.46143
8	15	90	0.26358	1.31597	3.16179
9	30	90	0.29134	0.99884	1.54544

Table 4.3 Strain rate during Tensile Test

Sl. No.	Overlapping Percentage (%)	Raster Angle (Deg)	Strain at Yield (%)	Strain at UTS (%)	Strain at Break (%)	Stress at Break (MPa)
1	0	0	0.70428	2.40297	6.21623	32.45842
2	15	0	0.79501	2.66902	2.77408	38.86602
3	30	0	0.96875	2.61100	2.69933	38.54854
4	0	45	0.77209	4.45063	9.34388	21.85857
5	15	45	0.88206	2.98461	6.47714	20.64598
6	30	45	0.957437	3.29354	5.47471	37.36047
7	0	90	0.80593	2.76305	4.27507	32.89687
8	15	90	0.73688	3.67897	8.83922	29.5432
9	30	90	0.84770	2.79588	4.02045	33.38998

4.3 Effect of overlapping percentage on the mechanical strength

Generally, increasing the path width can enhance the adhesion between layers. When the lines that are extruded are thicker, they have a larger surface area to bond with the layer beneath, resulting in improved adhesion. This improved adhesion can then lead to increased strength in the vertical direction (Z-axis). In the process of FDM printing, the mechanical strength of the printed object is typically higher in the X and Y directions (within the same layer) compared to the Z direction. Figure 4.2, 4.3, and 4.4 demonstrate the stress-strain curve at different path widths.

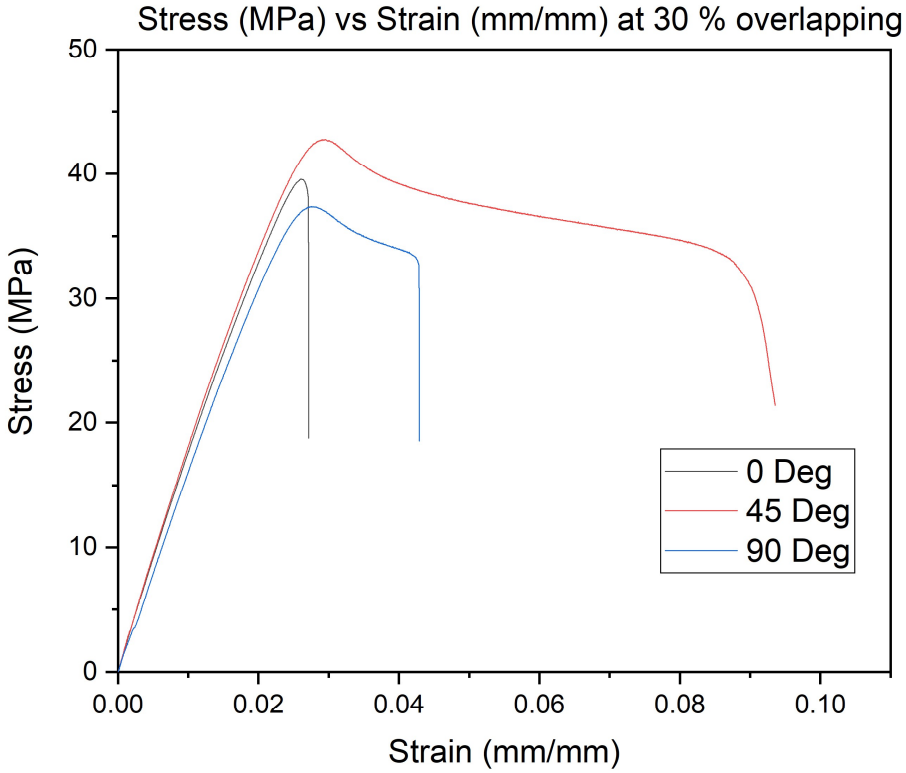

Fig. 4.2 Stress vs Strain at 30 % overlapping

Figure 4.2 illustrates the stress-strain relationship for 30% overlapping. The highest strength is achieved when the raster angle is 45°. The bonding strength between layers is greater in specimens with a raster angle of 45°. The anisotropic properties of printed samples and the flow of the filament have a positive effect on bonding strength. It has been observed that specimens with a raster angle of 45° degrees in relation to the loading direction are the strongest, and their strength decreases as the angle increases up to 90°. In the case of specimens with a 90° raster angle, the plastic region is greater compared to specimens with raster angles of 0° and 90° The different plasticity of the specimens can be attributed to filament flow and layer bonding strength. At 30 % overlapping the filament flow through the extrusion nozzle is not fine so there is a chance of heat trapping between two paths. It reduces the hardness. But in case of 45° raster angle the heat trapping is not so more as compare to anotherraster angle.

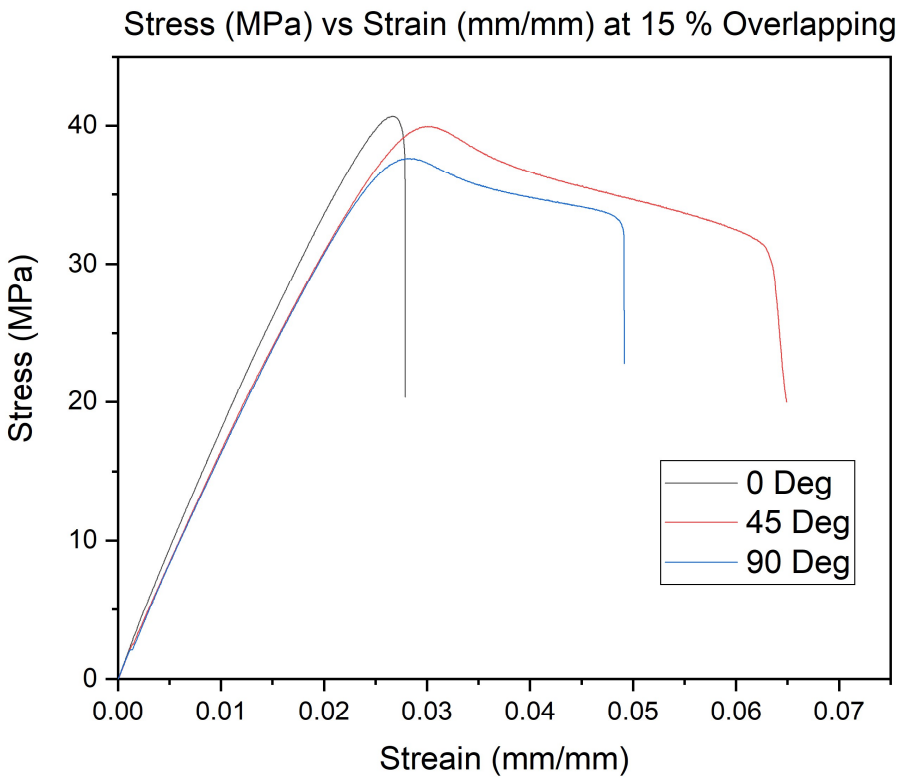

Fig. 4.3 Stress vs Strain at 15% overlapping

Figure 4.3 represents the stress-strain curve for 15% overlapping. If the overlapping percentage increases the UTS also increases due to more interlayer adhesion. But in here as overlapping percentage increases the UTS value also decreases. Base on toughness 45°raster angle specimen is more tough rather than0°raster angle specimen. At 0° raster angle the direction of applied force is longitudinal and the force is equally distributed into the specimen. At 15% overlapping 0° raster angle specimen gives maximum strength.

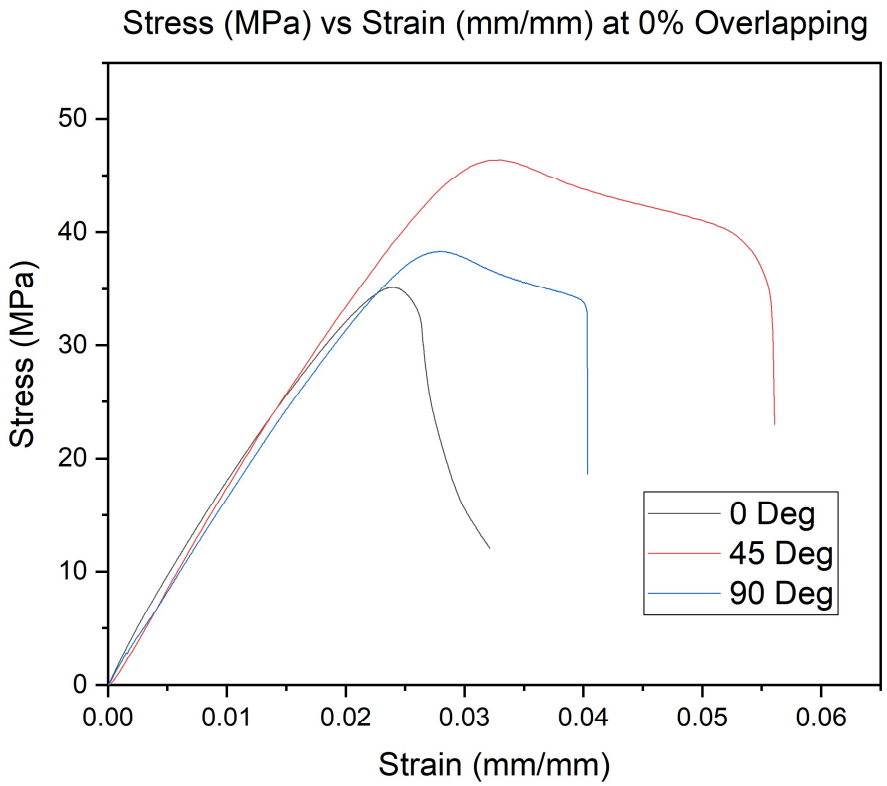

Fig. 4.4 Stress vs Strain at 0% overlapping

The stress-strain curve for a path width of 0% overlapping is shown in Figure 4.4. The plastic region is greater in the 45-degree path width specimen due to its strong layer bonding. The weight of 45° raster angle printed specimen is more than 0° and 90° raster angle printed specimen. Infill performance of 45° raster angle specimen is high. Due to more weight of specimen the density of fabricated specimen is high. So, the layer bonding or bonding strength also high as compare to others.

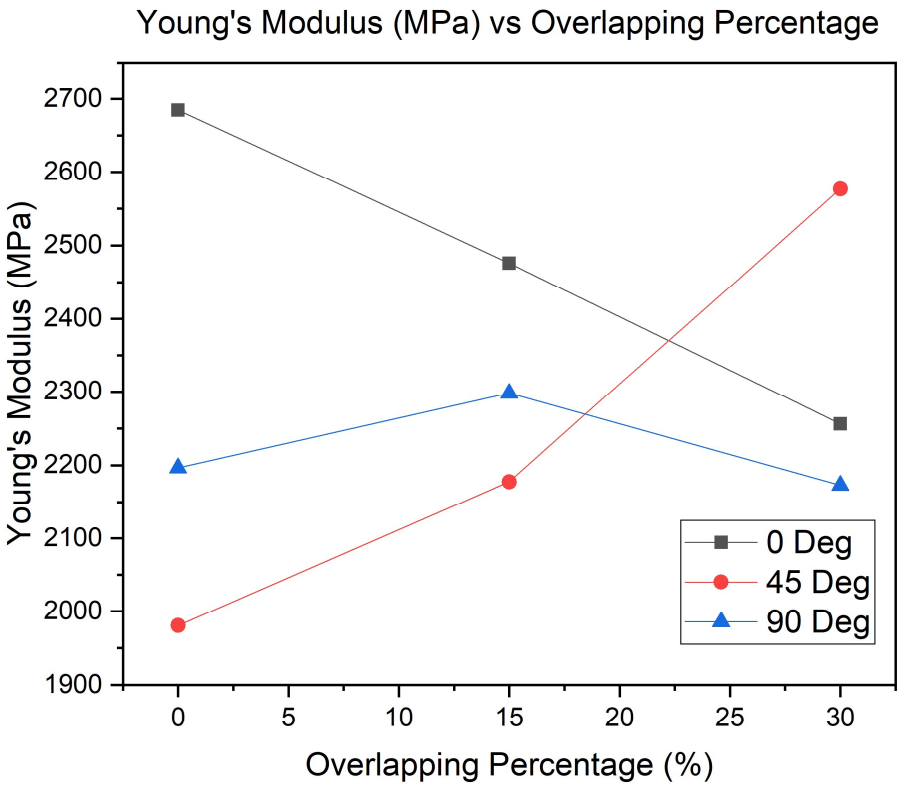

Fig. 4.5 Youngs Modulus vs Overlapping Percentage at different Raster Angle

Figure 4.5 depicts the curve of young's modulus versus path width at different raster angles. The young's modulus is high at a raster angle of 0° and 0% overlapping due to the specimen's anisotropy property and filament flow. Anisotropy property depends on change in build orientation. The orientation of the build heavily influences surface roughness. The lowest young's modulus is observed at 0% overlapping and a raster angle of 45°. As the overlapping percentage decreases the molten metal extruded from nozzle smoothly. As 0% overlapping no heat is trapped between two paths. So, the young's modulus is increasing as overlapping is decreasing for 0° raster angle.

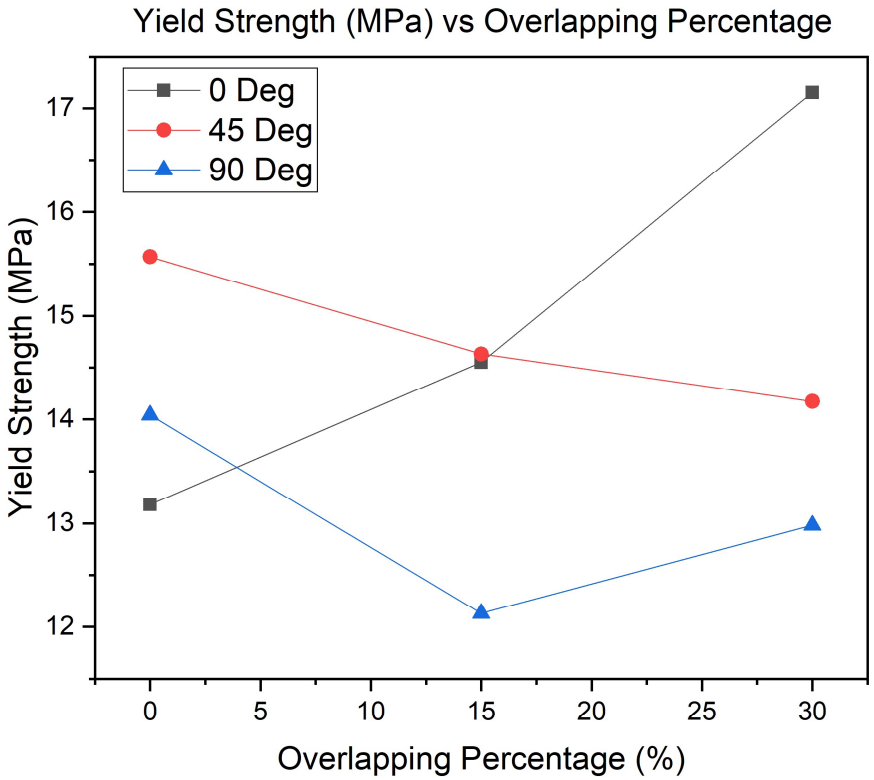

Fig 4.6 Yield Strength vs Overlapping Percentage at various Raster angle

Yield strength, an important mechanical property of materials, especially metals, refers to the maximum stress a material can endure before it undergoes permanent or plastic deformation. It plays a vital role in engineering design as it determines the safety and structural integrity of components and structures. Typically, yield strength is determined by conducting a tensile test, where a material sample is subjected to increasing tensile forces until it begins to deform plastically. Figure 4.6 displays the yield strength vs path width curve for various raster angles. In the case of a 0° raster angle, as the path width increases, the yield strength decreases due to elasticity. The load absorption capacity relies on factors such as layer bonding, layer overlapping, filament flow, and cooling. A higher overlapping of 30% results in a higher yield strength. For a 45° raster angle, the yield strength increases from a 30% overlapping to 0% overlapping width due to anisotropy property and filament flow. If the overlapping percentage is high, the filament flow becomes uneven, impacting the mechanical property of the fabricated specimen. For a 90° raster angle, as the overlapping percentage

decreases from 30% to 0%, the yield strength initially decreases and then increases. The highest yield strength is observed at 30 % overlapping with a 0-degree raster angle, while the lowest value is obtained when the overlapping is 30 % but the raster angle is 90 degrees. At 0° raster angle as the overlapping percentage decreases the overlapping area also decreases. Low overlapping area indicates low layer bonding strength. So, the yield strength at 0° raster angle specimens are in decreasing order. In case of 45° raster angle the overlapping percentage decreases the molten metal extruded from nozzle smoothly. As 0% overlapping no heat is trapped between two paths. So, the yield strength is increases at 45° raster angle.

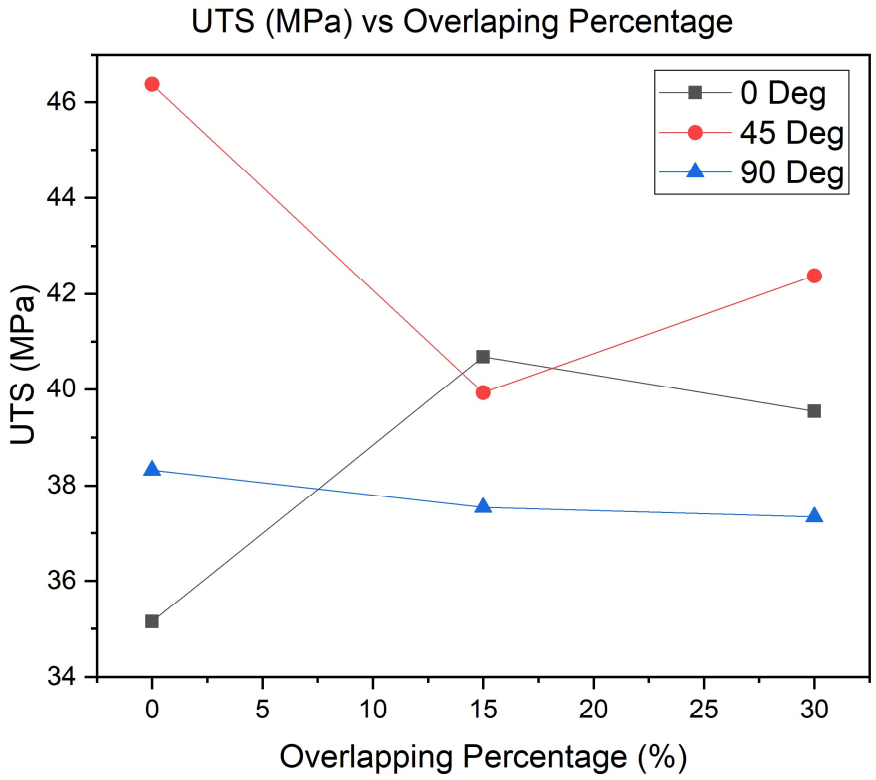

Fig. 4.7 UTS vs Overlapping Percentage at various Raster Angle

Ultimate Tensile Strength is a crucial characteristic for evaluating the strength and brittleness of materials. Figure 4.7 displays the UTS vs path width curve at different raster angles. During the initial stages of the tensile test, the material undergoes elastic deformation, meaning it stretches proportionally to the applied stress. However, as the stress increases, the material eventually experiences plastic deformation, resulting in permanent elongation. Eventually, the material reaches a point where it can no longer withstand the applied stress,

causing it to break. The maximum stress achieved just before the material breaks is known as the ultimate tensile strength. When the overlapping percentage varied from 30% to 0% at a 0-degree raster angle, the UTS initially increases due to good layer bonding at overlapping percentage of 15%. However, after reaching at 15% overlapping, the UTS decreases because a low overlapping percentage leads to poor interlayer adhesion. At a 45° raster angle, first the UTS valuedecreases from 42.38 MPa to 39.93 MPa then again increases up to 46.37 MPa as the overlapping percentage varies from 30 % to 0%. The overlapping percentage is low but UTS value is high due to low heat trapping between the two path increases the hardness value. Conversely, at a raster angle of 90° the UTS initially decreases as the overlapping decreases up to an overlapping percentage of 15%. However, the UTS then increases again due to an increase in hardness.

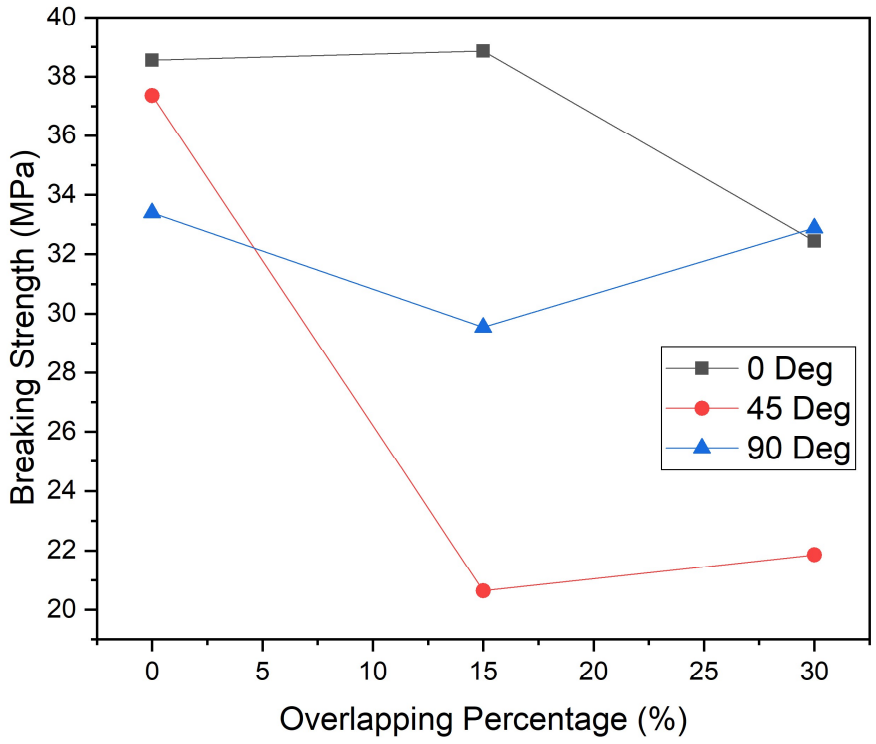

Fig. 4.8 Breaking strength vs path width at various raster angle

Breaking strength refers to the maximum force or load that a material or object can endure before it fails or breaks. The graph in Figure 4.8 illustrates the relationship between breaking strength and path width at different raster angles. Breaking strength is determined through

testing, such as a tensile test, where the material or object is subjected to gradually increasing force until it reaches the point of failure. At this point, the material or object is no longer capable of withstanding the applied force and fractures or breaks apart. When the overlapping percentage increases from 0% to 30%, the breaking strength initially increases slightly and then decreases. This is because increased overlapping leads to a lack of smooth filament flow, resulting in poor layer bonding strength. As a result of the low bonding strength, the material has a reduced capacity to absorb loads. At 45° and 90° raster angles, when the overlapping percentage decreases from 30% to 0%, the breaking strength initially decreases due to its anisotropic property, but then increases due to the filament flow direction and low heat trapping between two paths. Anisotropic property indicates different mechanical property at different build orientation. The maximum breaking strength is obtained at 0% overlapping and a raster angle of 0°, while the minimum breaking strength is observed at 15% overlapping and a raster angle of 90°.

4.4 Effect of raster angle on the mechanical strength

Figure 4.9, 4.10, and 4.11 represent the stress vs strain curve for different path widths. The impact of raster angle on the mechanical properties is explained below.

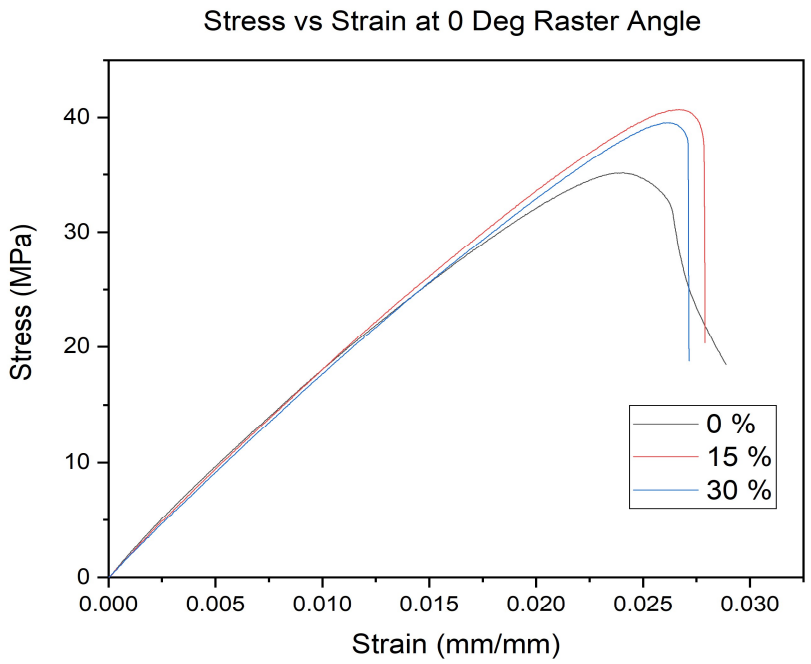

Fig. 4.9 Stress vs Strain at 0° Raster angle

Figure 4.9 illustrates the stress-strain curve at a raster angle of 0 degrees. The maximum strength is achieved in specimens with an overlapping percentage of 15% and a raster angle of 0 degrees. The bonding strength between layers is higher in specimens with an overlapping percentage of 15% due to its build orientation and interlayer adhesion for this overlapping. The anisotropic properties of printed samples, as well as filament flow and overlapping area, positively affect the bonding strength. It has been observed that the tensile strength increases up to a certain limit due to overlapping, and then it decreases. Up to a certain limit of overlapping the flow of extruded molten metal is smooth that helps to create high layer bonding strength. The maximum and minimum strength values are obtained at an overlapping percentage of 15% and 0%. In specimens with a no overlapping, resulting in lower layer bonding and bonding area. Therefore, specimens with a 0% overlapping have lower strength.

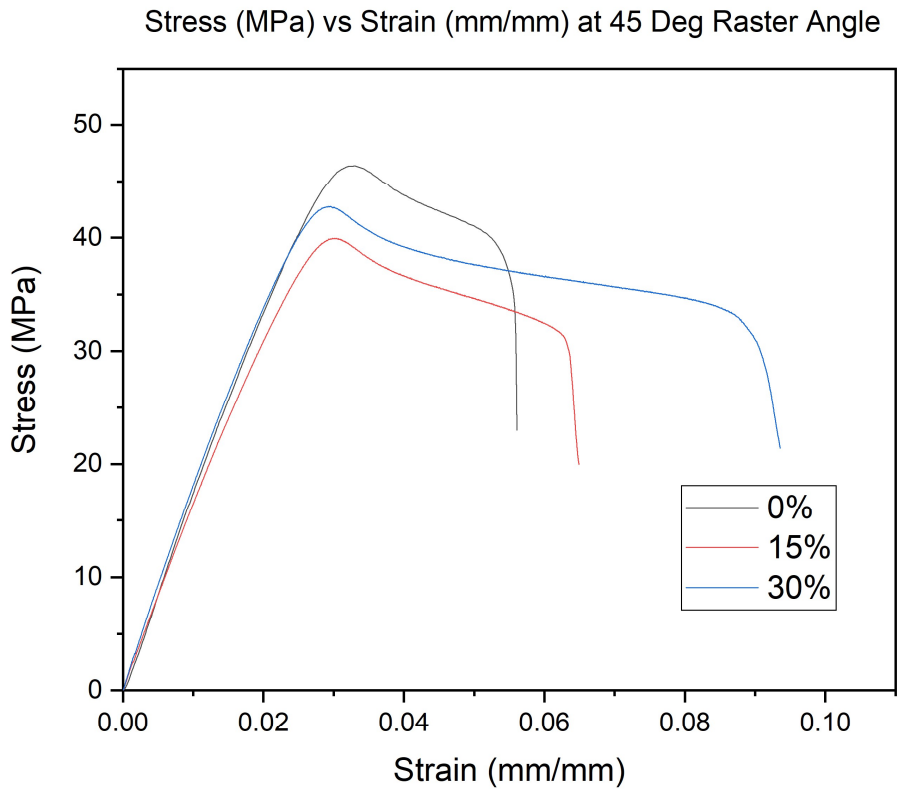

Fig. 4.10 Stress vs Strain at 45° Raster Angle

Figure 4.10 shows the stress vs strain curve at a 45° raster angle. Low heat trapped between the two pathscan increase their hardness. Increased hardness also leads to increased strength. In comparison to the other two printed specimens at the same raster angle, the specimen

without overlapping has greater tensile strength due to its build orientation. If the overlapping percentage increases the UTS value is also increases butat 45° raster angle as the overlapping percentage increases the UTS value is decreases because the molten material flow from the nozzle is not smooth when the overlapping percentage is increases at 45° raster angle. If the flow is not smooth then the track wise paths are unable to create a good interlayer bond between them.

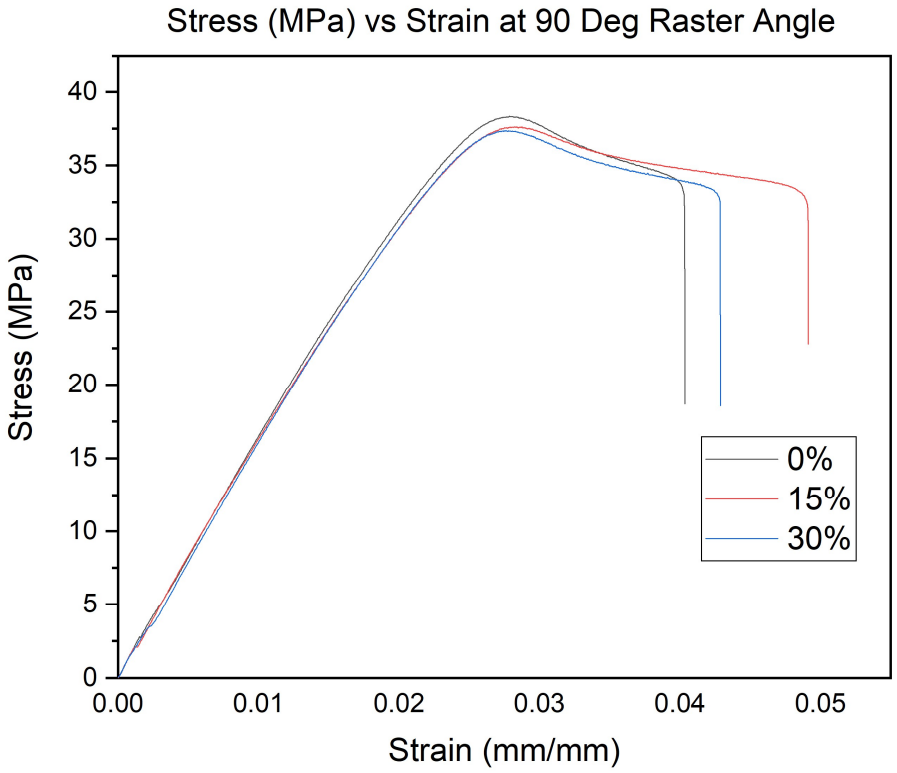

Fig. 4.11 Stress vs Strain at 90° Raster Angle

The stress-strain curve in Figure 4.11, at a 90° raster angle. Build orientation have an effect on mechanical properties of the printed part. As the overlapping percentage decreases then the overlapping area also decreases, it indicates high strength but due to build orientation and smoothly flow of molten material from extrudercan cause an effect. If the percentage of overlapping is increases then the flow of extruded material is not smooth. So, at 0% overlapping the maximum strength is obtained. It is challenging to determine which property has a greater impact on strength.

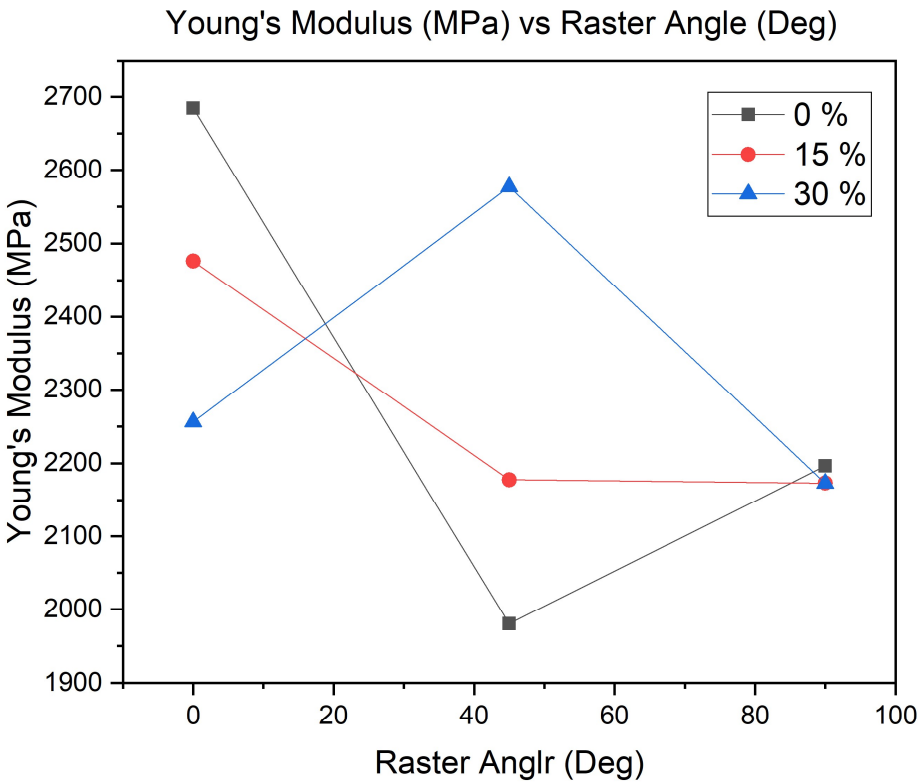

4.12 Young's modulus vs raster angle at various overlapping percentage

Polymers are generally more flexible and elastic, resulting in lower Young's modulus values. When the raster angle is changed from 0° to 90° with an overlapping percentage of 30%, the Young's modulus initially increases and then decreases. Build orientation indicates the direction of extruded materials flow. For overlapping percentage of 30% and 0%, the Young's modulus decreases up to 45° and then increases again. The decrease in Young's modulus is caused by build orientation, heat trapped between two paths followed by other factors.

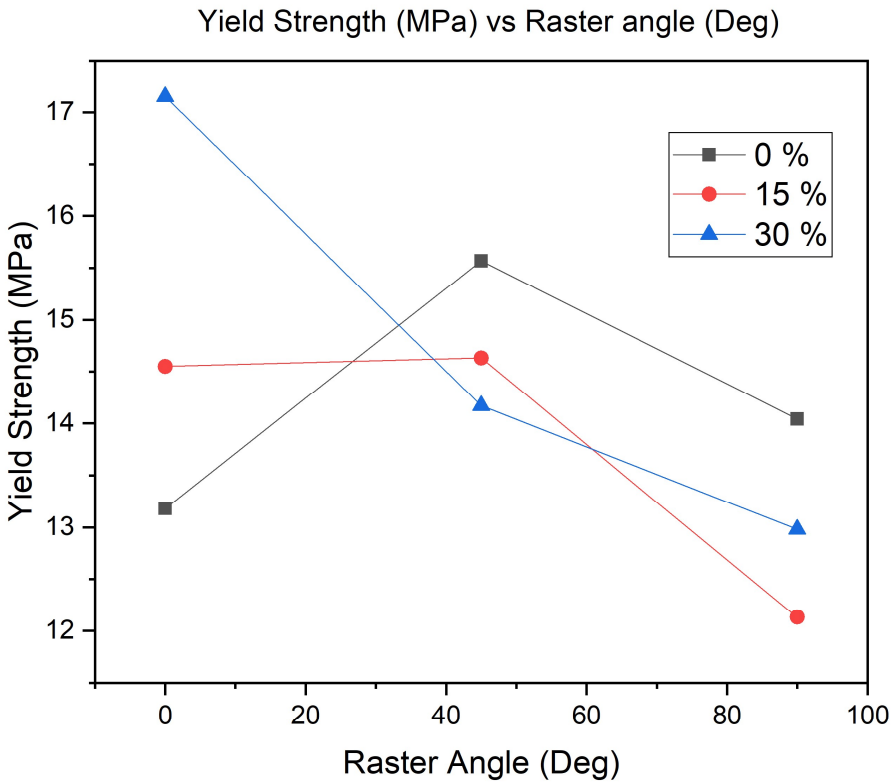

Fig. 4.13 Yield Strength vs Raster angle at various overlapping percentage

In Figure 4.13, the yield strength vs raster angle curve is shown for different path widths. As the raster angle increases, the yield strength decreases. This is because the build orientation and low due to the flow of the filament. When the overlapping is 15%, the yield strength initially increases up to a 45° raster angle and then decreases due to the performance of the interlayer bonding. At an overlapping of 0%, the yield strength increases as the raster angle increases up to 45°, but then decreases due to the material's anisotropy property and weak bonding between layers. The maximum yield strength of 17.15 MPa is achieved at a 0° angle and 30% overlapping, while the minimum yield strength of 12.14 MPa occurs at a 90° raster angle with an15% overlapping.

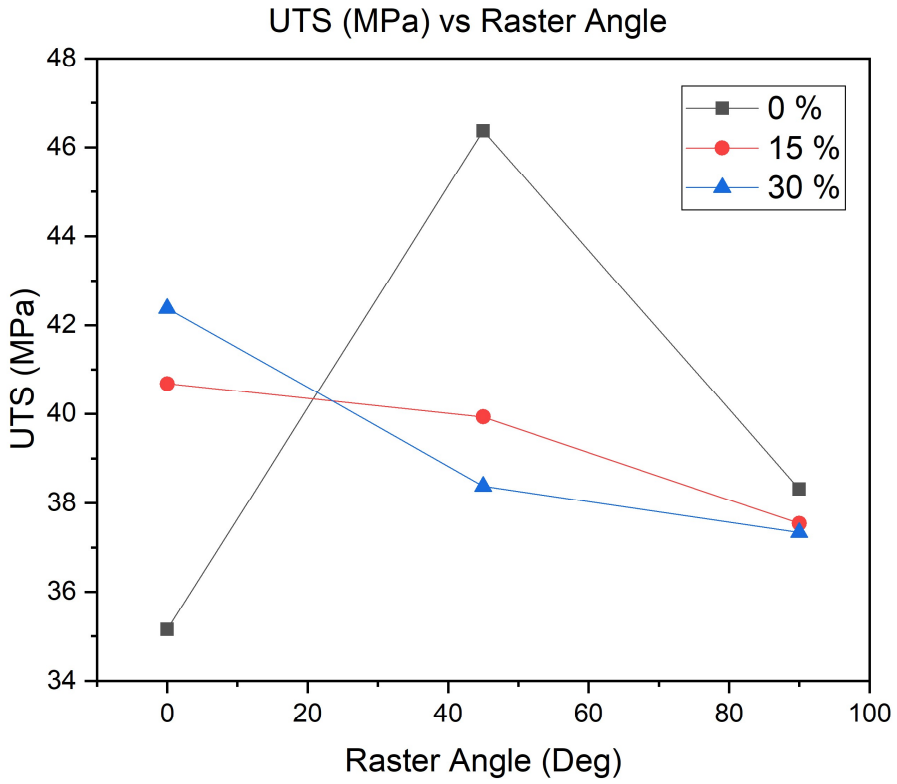

Fig. 4.14 UTS vs Raster Angle at different overlapping percentage

The maximum UTS is achieved at a 45° raster angle, while the minimum is at 0°. Increasing the raster angle reduces bonding strength, but other factors like interlayer adhesion, filament flow, and cooling contribute to the maximum UTS at 45°. Figure4.14 confirms that a 45-degree raster angle is advantageous for FDM 3D printing. The maximum and minimum UTS values are 46.37 MPa at 45 degrees and 35.16 MPa at 0°. Build orientation angle have an impact of UTS. This interlayer bonding and smoothly flow of extruded material influenced the build orientation or direction of printing. If there is an overlap but the extrude filament flow roughly then the bond between the two layer also decreases and this can defect the nozzle. In other hand when the overlapping percentage increases heat trapping between the two path also increases. This reduced the fabricated specimen hardness.

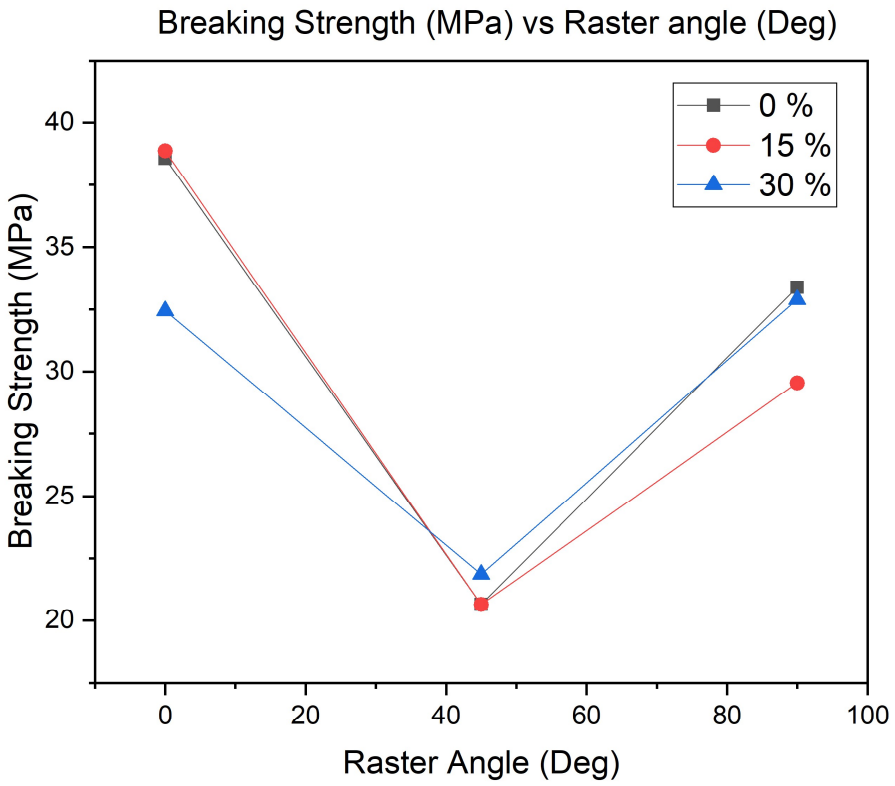

4.15 Breaking Stress vs Raster Angle at different overlapping percentage

Figure 4.15 illustrates the relationship between breaking stress and raster angle, specifically in relation to different overlapping percentage. As the raster angle increases, the breaking strength initially decreases until a 45° angle, after which it increases. Therefore, at a 0° raster angle, the maximum bending strength or interlayer adhesion is achieved, which then decreases and increases again at a 90 ° raster angle. The maximum and minimum breaking strengths occur at 0° and 45°, measuring 38.86 MPa and 20.64 MPa, respectively. The breaking point represents toughness. Consequently, specimens oriented with a 0° raster angle are tougher compared to those with 45° and 90° raster angles. The interlayer adhesion depends on the direction of extruded filament flow. At 0° raster angle the flow of extruded material is smooth. The heat trapping between the two layer is low.

CHAPTER V
CONCLUSIONS AND FUTURE WORK

5.1 Conclusions

This present study involves the fabrication of PLA samples (Type IV) with a thickness of 4.0 mm, following ASTM D 638, using Fused Deposition Modeling (FDM). The study focuses on investigating the effect of the printing process parameters, including overlapping percentage (0 %, 15 %, 30 %) and raster angles (0°, 45°, and 90°), on the mechanical properties of the specimens. The mechanical properties that are examined include Young's modulus, yield strength, tensile strength, and breaking strength.

According to the experimental data, the mechanical property of the fabricated sample is positively affected by the overlapping percentage and raster angle. The highest tensile strength of 46.37 MPa is observed when the raster angle is 45° and the overlapping percentage is 0%, while the lowest tensile strength of 35.16 MPa is observed when the raster angle is 0° and the overlapping percentage is 0%.

The breaking strength results indicate that the highest breaking strength (37.36 MPa) is observed when the raster angle is 45° and the overlapping percentage is 30%. Conversely, the lowest breaking strength of 20.64 MPa is observed when the raster angle is 45° and the overlapping percentage is 15%.

The results of the Young's modulus indicate that the highest value of Young's modulus, measuring 2297.83 MPa, is observed when the raster angle is set at 90° and the overlapping percentage is 15%. On the other hand, the lowest value of Young's modulus, measuring 1980.58 MPa, is observed when the raster angle is set at 45° and the overlapping percentage is 0%.

5.2 Future Work:

- **Material Characterization:** Further research can concentrate on comprehensively characterizing the material properties of PLA for FDM printing, including mechanical properties, thermal properties, degradation behavior, and long-term stability. By understanding how the material behaves in various processing conditions, it is possible to optimize FDM parameters more effectively and enhance the dependability of printed components.
- **Process Optimisation:** Future studies can explore advanced techniques for optimising the FDM process parameters specifically for PLA. This would involve examining how variables like nozzle temperature, bed temperature, layer height, print

speed, and cooling strategies affect the quality of prints and the mechanical properties of PLA parts. The objective would be to determine guidelines and suggestions for achieving the best printing conditions and improving the performance of PLA objects.

- **Mechanical Properties Analysis:** Further research can look into studying the mechanical properties of FDM-printed PLA parts in detail. This includes evaluating flexural strength, impact resistance, and fatigue properties.

References

1. Vaught, L.O., Polycarpou, A.A.: (2023) Investigating the effect of fused deposition modelling on the tribology of PETG thermoplastic. Wear 204736: 524-525.
2. Basha, S.M., Sankar, M.R., Venkaiah, N.: (2023) Experimental investigation on deballing and surface finishing of selective laser melted 18Ni300 steel using polymer rheological abrasive medium. Wear 523: 204813.
3. P. Herrera, P., Hernandez-Nava, E., R. Thornton, R., Slatter, T.: (2023) Abrasive wear resistance of Ti-6AL-4V obtained by the conventional manufacturing process and by electron beam melting (EBM). Wear 524-525: 204879.
4. Niu, F., Bi, W., Li, C., Sun, X., Ma, G.: (2023) TiC ceramic coating reinforced 304 stainless steel components fabricated by WAAM-LC integrated hybrid manufacturing. Surface & Coatings Technology https://doi.org/10.1016/j.surfcoat.2023.129635
5. Chen, F., Wang, Q., Zhang, Q., Huang, Z., Jia, M., Shen, Q.: (2022) Microstructures and mechanical behaviors of additive manufactured Inconel 625 alloys via selective laser melting and laser engineered net shaping. Journal of Alloys and Compounds 917: 165572.
6. Chen, F., Wang, Q., Zhang, C., Huang, Z., Jia, M., Shen, Q.: (2021) Organic mesh template-based laminated object manufacturing to fabricate ceramics with regular micron scaled pore structures. Journal of the European Ceramic Society 41: 2790–2795.
7. Lu, D., Zhang, L., Cheng, S., Zhang, K., Shao, W., Lin, D., Zeng, Z.: (2022) Microstructure control of SiCw/SiC composites based on SLS technology. Journal of the European Ceramic Society 42: 3747–3758.
8. Zhang, G., Song, D., Jiang, J., Li, W., Huang, H., Yu, Z., Peng, Z., Zhu, X., Wang, F., Lan, H.: (2023) Electrically assisted continuous vat photopolymerization 3D printing for fabricating high-performance ordered graphene/polymer composites. Composites Part B 250: 110449.

9. Liu, W., Song, H., Huang, C.: (2020) Maximizing mechanical properties and minimizing support material of PolyJet fabricated 3D lattice structures. Additive Manufacturing 35: 101257.

10. Shokraneh, S., Nojtahedzadeh-Faghihi, O., Amani, E.: (2023) A computational study of drop-on-demand liquid metal 3D printing using magnetohydrodynamic actuation. Additive Manufacturing 66:103462.

11. Tymrak, B.M., Kreiger, M., Pearce, J.M.:(2014) Mechanical properties of components fabricated with open-source 3-D printers under realistic environmental conditions. Materials and Design 58: 242–246.

12. Chacon, J.M., Caminero, M.A., Garcoa-Plaza, E., Nunez, P.J.: (2017) Additive manufacturing of PLA structures using fused deposition modelling: Effect of process parameters on mechanical properties and their optimal selection.Materials and Design 124: 143–157.

13. Alafaghani, A., Qattawi, A.: (2018) Investigating the effect of fused deposition modeling processing parameters using Taguchi design of experiment method. Journal of Manufacturing Processes 36: 164–174.

14. Yao, T., Deng, Z., Zhang, K., Li, S.: (2019) A method to predict the ultimate tensile strength of 3D printing polylactic acid (PLA) materials with different printing orientations. Composites Part B 163: (2019) 393– 402.

15. Alafaghani, A., Qattawi, A., Alrawi, B., Guzman, A.: (2017) Experimental Optimization of Fused Deposition Modelling Processing Parameters: a Design-for-Manufacturing Approach. Procedia Manufacturing 10: 791 – 803.

16. Raj, S.A., Muthukumaran, E., Jayakrishna, K.: (2018) A Case Study of 3D Printed PLA and Its Mechanical Properties. Materials Today: Proceedings 5: 11219–11226.

17. Miguel Fernandez-Vicente, M., Calle, W., Ferrandiz, S., Conejero, A.: (2016)Effect of Infill Parameters on Tensile Mechanical Behavior in Desktop 3D Printing. 3D Printing and Additive Manufacturing 3: 183- 192.

18. Johnson, G.A., French, J.J.: (2018) Evaluation of Infill Effect on Mechanical Properties of Consumer 3D Printing Materials, Advances in Technology Innovation 3: 179- 184.

19. Naik, M., Thakur, D.G., Chandel, S.: (2022) An insight into the effect of printing orientation on tensile strength of multi-infill pattern 3D printed specimen: Experimental study. Materials Today: Proceedings 62: 7391–7395.
20. Movrin, D., Luzanin, O., Plancak, M.: (2014) Effect of layer thickness, deposition angle, and infill on maximum flexural force in FDM-built specimens. Journal for Technology of Plasticity 39: 48-59.
21. Pernet, B., Nagal, J.K., Zhang, H.: (2022) Compressive strength Assessment of 3 D printing infill patterns.Procedia CIRP 105: 682–687.
22. Lee, J., Kwon, C., Yoo, J., Min, S., Nomura, T., Dede, E.M.: (2021) Design of spatially-varying orthotropic infill structures usingmultiscale topology optimization and explicit de-homogenization. Additive Manufacturing 40: 101920.
23. Jain, R., Gupta, N.:(2022) Design optimization of PLA lattice in 3D printing. Materials Today: Proceedings 59: 1577–1583.
24. Ambati S.S, Ambatipudi, R.: (2022) Effect of infill density and infill pattern on the mechanical properties of 3D printed PLA parts. Materials Today: Proceedings 64: 804–807.
25. Tanveer, Q., Mishra, G., Mishra, S., Sharma, R.: (2022) Effect of infill pattern and infill density on mechanical behaviour of FDM 3D printed Parts- a current review. Materials Today: Proceedings 62: 100–108.
26. Guajardo-Trevino, A.M., Ahuett- Garza, H., Orta-Castanon, P., Urbina-Coronado, P.D, Saldana, C., Kurfess, T.R.: (2022) Effects of deposition - strategy - induced rastergaps and infill voids on the compressive strength of 3D printed isogrid structures. Manufacturing Letters 31: 15–19.
27. Wang, K., Xie, X., Wang, j., Zhao, a., Peng Y., Rao, Y.: (2020) Effects of infill characteristics and strain rate on the deformation and failure properties of additively manufactured polyamide-based composite structures. Results in Physics 18: 103346.
28. Srinidhi, M.S., Soundararajan, R., Satishkumar, K.S., Suresh, S.:(2021) Enhancing the FDM infill pattern outcomes of mechanical behavior for as-built and annealed PETG and CFPETG composites parts. Materials Today: Proceedings 45: 7208–7212.
29. Ali, L.F., Raghul, R., Yogesh Murty Ram, M., Reddy, V.H., Kanna, N.S.: (2022) Evaluation of the polyamide's mechanical properties for varying infill percentage in FDM process. Materials Today: Proceedings 68: 2509-2514.

30. Abbas, T.F., Othman, F.M., Ali, H.B.: (2017) Effect of infill Parameter on compression property in FDM Process. Int. Journal of Engineering Research and Application 7: 16-19.
31. Sandhu, G.S., Boparai, K.S., Sandhu, K.S.: (2022) Influence of slicing parameters on selected mechanical properties of fused deposition modeling prints. Materials Today: Proceedings 48: 1378–1382.
32. Kumar, R., Ranjan, N.: (2022) Influences of infill percentage, bed temperature and outer perimeterson elongation of 3D printed nylon 6. Materials Today: Proceedings 48: (2022), 1661–1665.
33. Dharmalingam, G., Prasad, M.A., Salunkhe, S.: (2022) Investigation of impact strength at different infill ratesbiodegradable PLA constituent through fused deposition modelling. Materials Today:Proceedings 62: 551–558.
34. Gunasekaran, K.N., Kumaran, C.B.M., Madhankumar, K., Kumar, S.P.: (2021) Investigation of mechanical properties of PLA printed materialsunder varying infill density. Materials Today: Proceedings 45 :1849–1856.
35. Sukindar, N.A.B., Ariffin, M.K.A.B.M., Baharudin, B.T.H.T.B., Jaafar, N.A.B., Ismail, M.I.S.B.: Analysis on the Impact Process Parameters on Tensile Strength Using 3D Printer Repetier-Host Software. ARPN Journal of Engineering and Applied Sciences 12: 3341- 3346.
36. Luo,Y., Sigmund, O., Li, Q., Liu, S.: (2022) Topology optimization of structures with infill-supported enclosed voids for additive manufacturing. Additive Manufacturing 55:102795.
37. Rodríguez-Panes, A., Claver, J., Camacho, M.: (2018) The Influence of Manufacturing Parameters on the Mechanical Behaviour of PLA and ABS Pieces Manufactured by FDM: A Comparative Analysis. Materials 11: 1333.
38. Travieso-Rodriguez, J.A., Jerez-Mesa, R., Liuma, J., Traver- Ramon, O., Gomez-Gras, G., Rovira, J.J.R.: (2019) Mechanical Properties of 3D-Printing Polylactic AcidParts subjected to Bending Stress and Fatigue Testing. Materials 12: 3859.
39. Suteja, T.J., Soesanti, A.: (2020) Mechanical Properties of 3D Printed Polylactic Acid Product for Various Infill Design Parameters: A Review. Journal of Physics: Conference Series 1569: 042010.
40. Forster, W., Pucklitzsch, T., Dietrich, D., Nickel, D.: (2022) Mechanical performance of hexagonal close-packed hollow sphere infill structures with shared walls under compression load. Additive Manufacturing 59 :103135.

41. Farbman, D., McCoy, C.: (2016) Materials Testing Of 3d Printed ABS and PLA Samples to Guide Mechanical Design. Proceedings of the ASME 2016 International Manufacturing Science and Engineering Conference MSEC2016-8668.
42. Patil, P., Singh, D., Raykar, S.J., Bhamu, J.: (2021) Multi-objective optimization of process parameters of Fused Deposition Modeling (FDM) for printing Polylactic Acid (PLA) polymer components. Materials Today: Proceedings 45: 4880–4885.
43. Bachhav, C.Y., Sonawwanay, P.D.:(2022) Numerical comparison of additive manufacturing of ABS material based on infill design subjected to tensile load. Materials Today: Proceedings 62: 6727– 6733.
44. Majd, Y.F., Tsuzuki, M.S.G., Barari, A.: (2022) On the Accuracy of the Infill Pattern's Density in Additive Manufacturing. IFAC Papers Online 55: 43–48.
45. John, J., Devjani, D., Ali, S., Abdallah, S., Pervaiz, S.: (2022) Optimization of 3D printed polylactic acid structures with different infill patterns using Taguchi-grey relational analysis. Advanced Industrial and Engineering Polymer Research 6: 62 -78.
46. Yadav, D., Garg, R.K., Ahlawat, A., Phogat, A.: (2020) Optimization of FDM 3D printing process parameters for multimaterial using artificial neural network. Materials Today: Proceedings 21:1583–1591.
47. Doshi, M., Mahale, A., Singh, S.K., Deshmukh, S.:(2022) Printing parameters and materials affecting mechanical properties ofFDM-3D printed Parts: Perspective and prospects, Materials Today: Proceedings 50: 2269–2275.